Chapter 30
Intraperitoneal Chemotherapy

M. F. Flessner

For the nephrologist, the major therapeutic use of the peritoneal cavity is dialysis, but the peritoneum is a portal of entry for a wide variety of local and systemic therapies. Because of intravenous access problems in neonates, transfusion of packed red blood cells was one of the earliest uses of intraperitoneal (i.p.) therapy [1, 2]. Insulin is often placed in the dialysate in order to treat glucose intolerance during peritoneal dialysis [3], and i.p. insulin delivery is currently undergoing investigation as a means of long-term therapy in diabetes [4–6]. Erythropoietin, prescribed as replacement therapy for the anemia related to end-stage renal disease (ESRD), has been administered intraperitoneally [7, 8]. In contrast to these forms of i.p. therapy, which are designed to treat systemic illnesses, antibacterial agents are injected intraperitoneally in order to treat peritonitis [9]. In the past 20 years, i.p. chemotherapy has increasingly been evaluated for treatment of malignancies localized to the peritoneal cavity [10–29].

Since i.p. therapy is more cumbersome than systemic, intravenous (i.v.) delivery, the critical point that the clinician must determine is the usefulness of such an approach. Is there a pharmacokinetic advantage of administering the drug regionally (i.p.) versus systemically? In other words, does the drug achieve therapeutic concentration in the region of interest while maintaining an acceptably low level in the general circulation and thereby minimize toxicity? The i.p. administration of a drug such as erythropoietin, which has a site of action in the bone marrow and not the peritoneal cavity, may not be an appropriate use of this route. Because of a slow rate of systemic absorption, very large concentrations of erythropoietin must be injected with the peritoneal dialysate to attain levels in the blood which are equivalent to those attained with i.v. or subcutaneous (s.c.) dosing. Much of this expensive agent must be wasted, since the solution must be drained from the patient before the drug is fully absorbed [7].

What follows is an analytical approach to the evaluation of the i.p. route of administration with respect to the i.v. route. The approach assumes that the target of the therapy is either a cellular component in the peritoneal cavity (bacteria or tumor ascites cells) or the tissues surrounding the peritoneal cavity. The properties of the target significantly influence the method of delivery and the feasibility of the technique.

Pharmacokinetic Advantage

At steady state, the quantitative formula for pharmacokinetic advantage (R_d) for a target within the peritoneal cavity is in its simplest form [30]:

$$R_d = \frac{\left(\frac{C_P}{C_B}\right)_{i.p.}}{\left(\frac{C_P}{C_B}\right)_{i.v.}} \quad (1)$$

where: C_P = concentration in the peritoneal cavity, C_B = concentration in the systemic circulation, and the subscripts indicate the route of administration. In planning a therapeutic strategy the physician would like to predict R_d prior to administration of the drug in humans. The pharmacokinetics of a particular drug are based on the transport physiology of the region in which it is administered, as well as pharmacokinetic processes in the rest of the body.

M.F. Flessner (✉)
University of Mississippi Medical Center, Jackson, Mississippi
e-mail: mflessner@umsmed.edu

R. Khanna, R.T. Krediet (eds.), *Nolph and Gokal's Textbook of Peritoneal Dialysis*,
DOI 10.1007/978-0-387-78939-2_30,

Multicompartmental Concept

Physiologic characteristics of the peritoneal cavity, which cause it to be advantageous for removal of waste metabolites and poisons from the body, also provide an excellent portal of entry into the body for many drugs. The tissue space surrounding the cavity is capable of absorbing almost any agent including cell size materials placed in the cavity. Fig. 30.1 illustrates the complexity of the peritoneal cavity, in terms of pharmacokinetic pathways. Solute and fluid transfer as indicated from the peritoneal cavity occurs into the various tissues surrounding the cavity and from there into the body compartment via the circulation. Although all surfaces are potentially targets for any drug or agent within the peritoneal cavity, the relative importance of a specific area is determined by whether the surface is in contact with the fluid in the cavity. This issue is particularly important in the regional administration of antineoplastic agents and will be discussed below.

In Fig. 30.1, the peritoneal tissue has been divided into four major compartments. Each of these compartments receives blood originating in the body compartment. The blood flows through capillary exchange vessels distributed throughout the tissue and returns to the body compartment. Lymph flows from each tissue space to the body compartment as illustrated in Fig. 30.1. Each tissue compartment receives solutes from the peritoneal cavity with a solute mass transfer rate of S and fluid at rate F (S and F are illustrated as positive from the cavity into the tissue).

The body is shown as a single compartment in Fig. 30.1, but it could be represented by multiple compartments, if the pharmacokinetic characteristics of the drug demand it. For example, a drug that has its major effect or chief site of metabolism in the liver would be a candidate for such a model, in which the relative rates of absorption into each tissue would determine the overall effectiveness of the medication. The volume of the body compartment equals the volume of distribution of the drug in the total body excluding the tissues surrounding the peritoneal cavity. Its concentration is assumed to equal the arterial concentration. The drug is cleared at some rate CL_{BC} and there may exist some rate of input into the compartment (I_{BC}). Blood flows from the body compartment through each peritoneal compartment with rate Q_i. Lymph flows from each organ system (L_i) through two major systems into the body compartment: the thoracic duct (L_{TD}) and the right lymph duct (L_{RLD}).

The peritoneal cavity compartment is assumed to be well mixed; i.e., the concentration is the same throughout the cavity. The cavity may have a solute input rate of I_{PC} and a drainage rate of D_{PC}. The cavity does not exchange directly with the body compartment; transport occurs only with the tissue compartments.

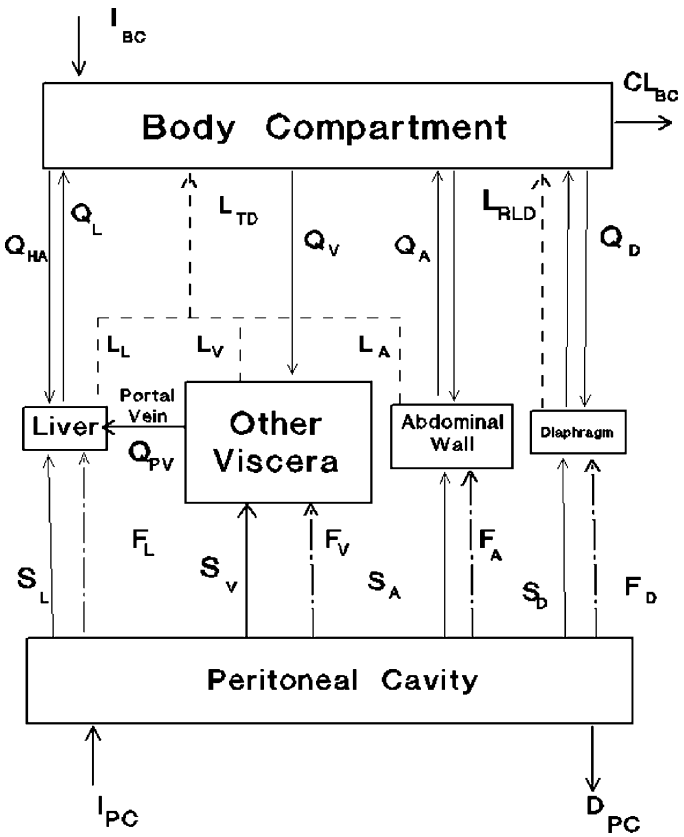

Fig. 30.1 Compartmental model concept of intraperitoneal drug delivery in which transport occurs between the cavity and specific tissues surrounding the cavity. *Symbols*: I = infusion; CL = clearance; D = drainage from the cavity; Q = blood flow through organ or vessel; L = lymph flow from tissue to body compartment; F = rate of convection from the cavity to tissue; S = rate of solute transfer from the cavity to tissue. *Subscripts*: A = abdominal wall and psoas; BC = body compartment; D = diaphragm; HA = hepatic artery; L = liver, PC = peritoneal cavity; PV = portal vein; RLD = right lymph duct; TD = thoracic duct; V = other viscera including the intestines, stomach, pancreas, and spleen. See text for a full description

The diaphragm is included as a separate compartment because of the specialized subdiaphragmatic lymphatic system [31, 32], which accepts cell sizes to 25 μm in diameter [33] and which accounts for 70–80% of the total lymph flow from the cavity [34–36]. The diaphragm also experiences relatively large but variable hydrostatic pressure gradients during respiration, because of its position between the thoracic and abdominal cavities. Expiration facilitates direct fluid movement into the diaphragmatic interstitium and into the lacunae of the subdiaphragmatic lymphatic apparatus [31, 32].

The abdominal wall is shown as a separate compartment because it is the single largest recipient of fluid transfer from the cavity. The abdominal wall is of major importance as well because it is likely that much of the solute transfer flows through this tissue due to contact with the fluid [37]. In animal experiments this amounts to 40–50% of the total fluid movement out of the cavity [35, 38, 39]. The reason for this fluid movement has been attributed to the hydrostatic pressure gradient across the abdominal wall. In addition, the lymphatics are not well developed in this tissue and therefore do not provide the safety valve that they do in intestinal tissue [40]. Proteins or other macromolecular drugs, which are carried into the muscle tissue as a result of the hydrostatic pressure-driven convection will transfer to the body compartment slowly [38, 41, 42].

The liver is separated from the other visceral tissues because of its unique portal circulation coupled with its role in drug metabolism. The liver may be primarily responsible for protein losses into the cavity.

The "other viscera" include the spleen, stomach, intestines, and the pancreas, which are lumped together in a single tissue compartment. The viscera present the largest portion of the peritoneal surface area, but it is unknown at this time how much of this surface area is in contact with the fluid at any time during a therapeutic treatment. As drugs transport into the tissue from the cavity they will also be taken up by the networks of vessels within each of these tissues and then return to the general circulation. The rate of the drug transfer to the blood is governed by diffusion and convection (solvent drag) within the tissue space, the permeability-surface area density of the blood exchange vessels, and the rate of blood perfusion. The process of drug uptake from the peritoneal cavity includes the same physiological mechanisms responsible for transport during dialysis except that the direction of transport is reversed.

Table 30.1 lists the human parameters, which are independent of solute size but are necessary to solve the system in Fig. 30.1. The first two columns concern peritoneal surface area. The first column specifies the percentage of the total peritoneal surface area, while the second tabulates the total surface area in cm^2. The data of Rubin et al. [43] are used because the measurements were more conservative than those of Esperanca and Collins [44], since the mesentery was not included. The areas have been scaled to a 70 kg body weight by the factor $(\text{body weight})^{0.7}$ [30]. It should be noted that these are total surface areas that have resulted from the dissection of each tissue and its surface area measured by planimetry; these area values may not represent the true area of contact between the peritoneal fluid and the tissue.

The tissue weights were estimated as follows. The liver weight was taken directly from a table in Ludwig [45]. The "other viscera" weight was computed from the sum of the spleen (0.14 kg) and intestines. The latter were estimated from the product of the total surface area [43], the average thickness of 2.5 mm [46], and the specific gravity of these tissues, which was assumed to equal 1 g/cm^3. The thicknesses of the abdominal wall and diaphragm were estimated to be 2 cm and 0.3 cm [47], respectively, and the tissue weight was calculated in the same fashion as in the case of the hollow viscera.

There have been a number of estimates of the rate of perfusion (q_i) of the abdominal tissues. Measurements in the control animals [48] for the parietal wall (0.06 mL/min/g tissue) and diaphragm (0.31) are listed in Table 30.1. Other estimates [49] for the parietal wall tended to be much higher, because of the specific preparation and use of vasodilators. The perfusion rates in the "other viscera" and the liver (includes both hepatic artery and portal flow) can be estimated from total organ blood flows [50, 51] and divided by the weight of each system. The estimates for the gastrointestinal tract agree with several other measurements made in a variety of tissues from other species [52–54]. The total blood flows for the diaphragm and abdominal wall (Q_i) can be calculated from the product of the organ weight and q_i.

Table 30.1 Adult human parameters which are independent of solute size (scaled to 70 kg body weight)

Tissue	Percentage total surface area	A_i (cm^2)	Weight (g)	q_i (mL/min/g)	Q_{tot} (mL/min)	L (mL/min)	F (mL/min)	L/F
Liver	13.2	1056	1800	0.83	1500	0.46	0.07	6.83
Other viscera (intestines spleen, stomach)	67.9	5432	1700	0.65	1100	0.97	0.33	2.91
Abdominal wall	11	880	1960	0.06	118	0.04	0.67	0.05
Diaphragm	7.9	632	190	0.3	57	0.27	0.27	1.01

Thoracic duct lymph flow has been measured in humans and typically has a flow rate of 1–1.6 mL/h/ kg body weight [55, 56]. Nonruminant animals have flow rates on the order of 2–3 mL/h/kg body weight [35, 57–59]. Morris [57] estimates that the contributions of the liver and gastrointestinal tract amount to 30% and 64%, respectively, of the thoracic duct flow. The remaining 6% of the total flow is from all the skeletal muscle below the diaphragm, including the psoas, the abdominal wall, and the lower limbs. In order to estimate the lymph flow for humans, the mean value for the thoracic duct (1.3 mL/h/kg body weight) was multiplied by the percentages obtained by Morris for each organ system: 30% for liver and 64% for other viscera. One-third of the remaining 6% was arbitrarily assumed to be the contribution of the abdominal wall. Total lymph flows were then calculated by multiplying each tissue-specific lymph flow rate by the body weight (70 kg) and converting to mL/min.

Of the lymph that exclusively leaves the peritoneal cavity, 70–80% occurs through the subdiaphragmatic system [34]. This is a major site for transport of fluids, macromolecules, and cellular materials from the cavity to the blood. Values for flow range from 0.6–1.8 mL/h/kg body weight in the anesthetized rat [35] to 0.1 mL/h/kg in anesthetized sheep and 0.50 mL/h/kg in awake sheep [60]. Flow rates in awake, healthy continuous ambulatory peritoneal dialysis (CAPD) patients vary from 0.14 to 0.28 mL/h/kg body weight [54, 55]. The rates appear to increase in cirrhosis to 0.43 mL/h/kg [56]. We have chosen the mean rate of 0.23 mL/h/kg and multiplied it by 70 kg to find the diaphragmatic lymph flow rate of 16.1 mL/h.

The next to last column in Table 30.1 lists estimated total flow rates of fluid in mL/min to each organ system. The total flow from the cavity has been estimated from the average of three studies in healthy CAPD patients [53–55, 57] to be 1.33 mL/min. This flow is driven by the hydrostatic pressure in the cavity [29, 58, 59] and occurs in the face of hyperosmolar solutions, which draw fluid into the cavity [31, 33, 59–61]. These studies have shown that protein acts as a marker for fluid movement. The total hourly flow rate has been partitioned to each set of tissues on the basis of the fraction of protein deposition from the cavity of the rat [31] with corrections for the rates of lymph flow from each tissue.

Blood Flow: Does It Limit Solute Transfer?

Estimates of the effective blood flow surrounding the peritoneal cavity suggest that transport between the blood and the cavity is not limited by the supply of blood, except in cases of severe hypotension. Physiologists have attempted to estimate the "effective" blood flow by measuring the clearances of various gases from the peritoneal cavity, assuming that these were limited by blood flow only. Gas clearances of hydrogen [61, 62] and CO_2 [63] have been determined in small mammals and found to be equal to 4–7% of the cardiac output. However, this method of determining the effective peritoneal blood flow may actually underestimate the true blood flow. Collins [64], who studied absorption of several inert gases from peritoneal gas pockets in pigs, found almost a three-fold range in clearance, which correlated with the gas diffusivity in water. If the transport of these gases was limited by blood flow, the clearance of each gas would have been the same. The results imply that the transport of these gases is not limited by blood flow but by resistance to diffusion in the tissue. Gas clearance data therefore underestimate the true peritoneal blood flow, and the conclusion, based on lumped clearance data, would be that blood flow limitation in the peritoneal cavity is unlikely.

The lumped clearance argument, however, does not rule out specific limitations in a portion of the peritoneal cavity, which may be offset by another set of tissues. To investigate the possibility of blood flow limitation of transport across specific surfaces of the peritoneum, the chamber technique was utilized to answer the question of "local" limitations of blood flow on urea (which should diffuse rapidly due to its small molecular weight and which would be more likely to demonstrate blood flow limitations) transport across the liver, stomach, cecum, and abdominal wall [65]. The mass transfer rates of urea were determined under conditions of control blood flow, blood flow reduced by 50–80%, and no blood flow (postmortem); the blood flow was monitored simultaneously with laser Doppler flowmetry. While all four tissues showed marked decreases in urea transport after cessation of blood flow, only the liver displayed a decrease in the rate of transfer during periods of reduced blood flow. Further studies with the chamber technique tested the effects of blood flow on osmotically induced water flow from the same four tissues; results demonstrated statistically nonsignificant decreases in water flow in the cecum, stomach, and abdominal wall [66]. Analogous to the solute data, the liver demonstrated a significant drop in water transfer with reduced blood flow. Thus, transport of both solute and water across the surface of the liver is limited by blood flow. Zakaria and co-workers [67] have shown in rats that the liver is responsible for only a very small amount of the actual area of transfer; this implies that a drop in blood flow to the liver would have minimal effects on overall transperitoneal transport. These data support and extend earlier studies of peritoneal dialysis in dogs [68] and rats [69] during conditions of shock and demonstrate relatively small changes in solute transfer. These all support the use of the technique for solute or fluid removal during periods of low systemic blood pressure and the probable low blood perfusion of the organs surrounding the peritoneal cavity.

Simplified Compartmental Model

The Problem of Surface Contact Area

The area of the peritoneum in contact with the therapeutic solution is typically a fraction of the anatomic area. Research in animals [37, 70] and humans [71, 72] has clearly demonstrated that during dialysis only about 30% of the total surface area is covered at any one time. Although over 24 h, the entire peritoneum will make contact with an i.p. solution [37], the duration of contact with specific parts of the peritoneum is unknown. Dialysis solutions containing glucose are gradually absorbed from the cavity and, therefore, there is a receding volume and contact surface area after the effective osmolar gradient is lost. An alternative to the typical dialysis solution is one containing 4% of icodextrin (a 20 to 30 kDa starch), which has been shown to maintain the peritoneal volume at a constant for up to 48 h [73], with a loss of 50% over the next 48 h. A 7.5% icodextrin solution has been shown to be effective as a drug carrier for 5- fluorouracil [74] for up to 96 h; this type of solution maintains the volume and the area of contact relatively constant. However, even the icodextrin solutions do not guarantee contact with the target areas for any given length of time. The volume of the solution, the size of the patient, and the patient's position all affect the peritoneal contact area. For example, if the patient is ambulatory, even a large volume (3 L) may pool in the bottom of the peritoneal cavity. Large portions of the peritoneum may not be covered [37], and therefore the residence time of the medication may be a problem for certain regions of the cavity.

The lack of certainty about the surface contact area and the residence time at each tissue surface complicates the implementation of the multicompartmental model of Fig. 30.1. There are just no data on which to base a weighting system for fluid contact to a particular tissue. In addition, research in animals has demonstrated that for small molecules (~500 Da), the relative permeability of visceral and parietal peritoneal surfaces are nearly the same [75]. For many substances, the model concept of Fig. 30.1 requires many defined parameters, and a simpler approach can be employed to calculate R_d. A number of examples will follow the simplified theory. While Eq. 1 can also be applied to the treatment of malignant ascites, its use in treating metastatic tumor implants is complicated by the altered tumor properties that impact the penetration and effectiveness of the agent.

Simplified Model Concept

The model concept presented in Fig. 30.2 is a simple, two-compartmental approach, without regard to the anatomy and physiology of the system. It is the most straightforward concept to estimate the R_d from Eq. 1. The body consists of two compartments: 1) the systemic blood circulation that circulates through the drug's volume of distribution (V_D) and 2) the peritoneal cavity where the therapeutic drug is in solution. The transfer of drug across the so-called "*peritoneal membrane*" is modeled as a simple transfer of mass as follows:

$$\text{rate of mass transfer} = \frac{d(C_P V_P)}{dt} = -MTAC(C_P - C_B) \tag{2}$$

where MTAC = the overall mass transfer-area coefficient for the drug or solute, C_P = the concentration in the peritoneal cavity, V_P = the volume in the peritoneal cavity, and C_B = the concentration in the blood. A mass balance on the blood yields:

$$\frac{d(C_B V_D)}{dt} = MTAC(C_P - C_B) - CL_{BC}(C_B V_D) \tag{3}$$

where CL_{BC} = the total body clearance, which is often approximated by the glomerular filtration rate divided by V_D for unbound, water-soluble drugs. Fig. 30.3 provides MTACs for water-soluble drugs in normal dialysis patients and in patients undergoing i.p. chemotherapy [76–78]. These may underestimate or overestimate the mass transfer of particular drugs in tumor-bearing patients. As can be seen in Fig. 30.3, the MTAC for heated drugs is considerably higher than the nonheated solutions [79–81]. This likely due to the combination of vasodilation with increased peritoneal blood flow and greater surface contact area with the use of dual catheters and a continuous flow system. The area is not well defined in these perioperative procedures, but the technique can significantly enhance the pharmacokinetic advantage and the efficacy [82]. Drugs that are more lipid soluble will have an order of magnitude higher rate of clearance from the peritoneal cavity [83–85].

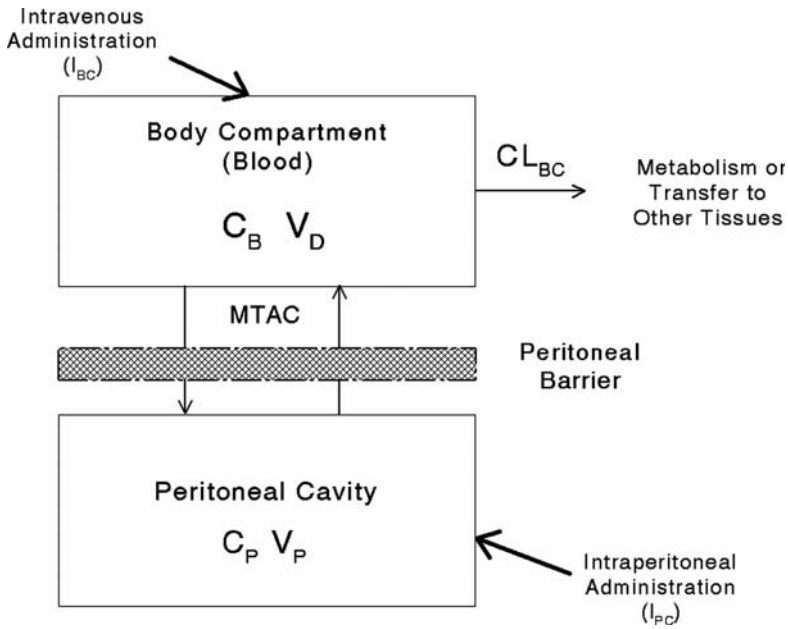

Fig. 30.2 Simplified two-compartment model. Nomenclature is the same as in Fig. 30.1. MTAC = mass transfer-area coefficient; C_B = concentration in blood; V_D = volume of distribution for drug in body compartment; C_P = concentration in peritoneal cavity; V_P = volume in peritoneal cavity. See text for details

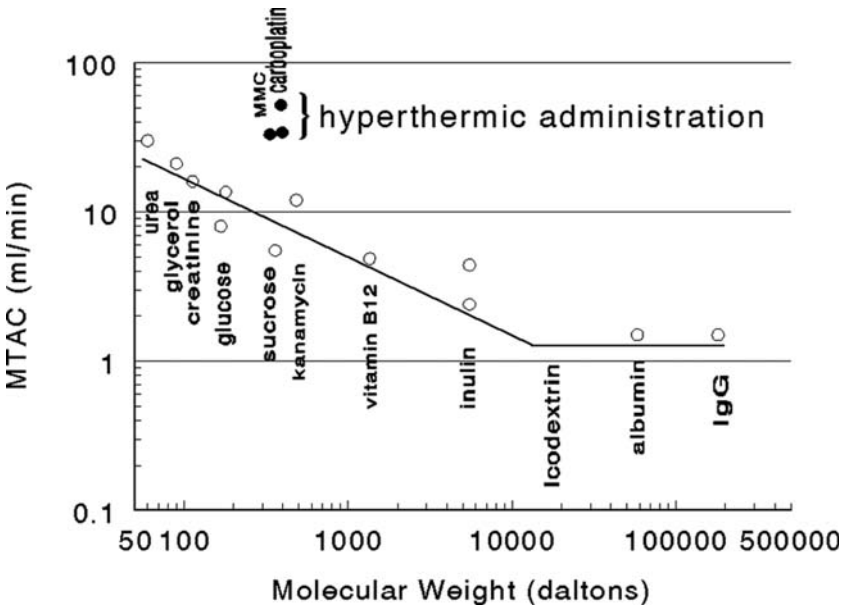

Fig. 30.3 Mass transfer-area coefficient (peritoneal clearance) versus molecular weight

Variation of MTAC with Body Size

Figure 30.4 shows the clearance (~MTAC) for urea and inulin for the rat, rabbit, dog and human; these species cover a body-weight range from 200 g to 70 kg [30]. The parameter increases as the 0.62–0.74 power of body weight for inulin and urea, respectively. The average of these two values is very close to the two-thirds expected for body-surface-area scaling. Keshaviah and colleagues [82] demonstrated a linear correlation between the volume at which MTAC was maximum and the body surface area in a study of 10 patients with body surface areas ranging from 1.4 to 2.3 m^2. Since the characteristic time for absorption from the peritoneal cavity is equal to V_P/MTAC, similar time scales can be

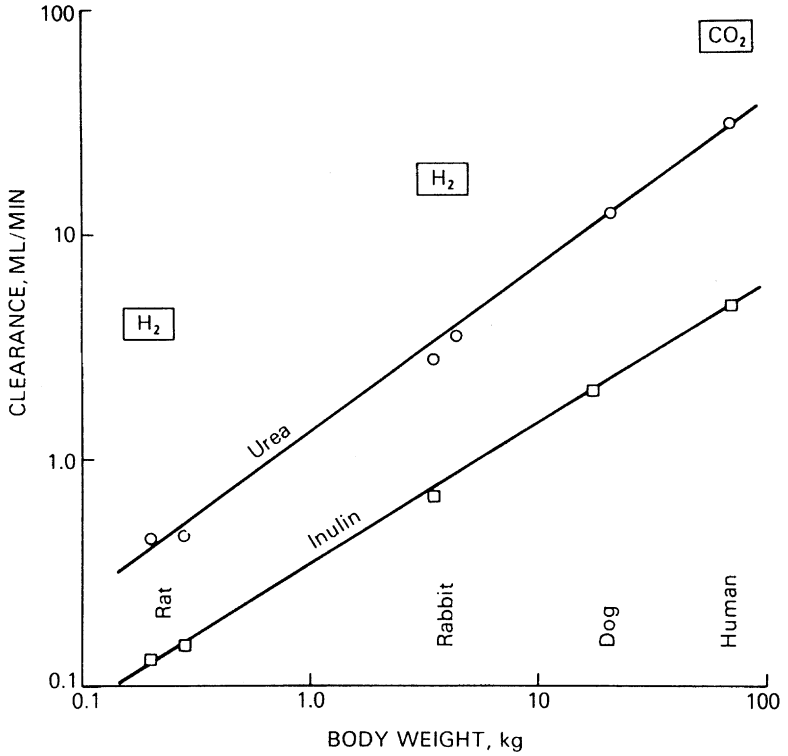

Fig. 30.4 Peritoneal clearance (or mass-transfer-area coefficient) for the indicated gases, urea, and inulin versus body weight. From [116]

achieved in humans and experimental animals if the volume is scaled as the two-thirds power of the body weight. For example, 2 L in the peritoneal cavity of the 70 kg human patient (29 mL/kg) would be equivalent to 40 mL in a 200 g rat (200 mL/kg) because $(200/70{,}000)^{2/3}$ (2,000) = 40. These scaling criteria permit the design of experiments, which more accurately reflect in small animals dialysis that is carried out in humans.

Calculation of the Pharmacokinetic Advantage

The solution of Eqs. 2 and 3 requires the parameters of V_D, CL_{BC}, and the MTAC for each solute and the doses to be given (dose = $C \times V$ for each compartment), which are given i.v. or i.p. at time = 0. The concentration versus time may then be calculated in each compartment for each route of administration; these concentrations define the R_d.

Alternatively, if a drug is infused at a constant rate into a fixed volume of fluid in the peritoneal cavity until steady state is achieved, then a regional advantage will be observed:

$$R_{\text{i.p.}} = (C_P/C_B)_{\text{i.p.}} \tag{4}$$

Similarly, if the drug is infused at a constant rate intravenously with the same fixed i.p. volume of fluid, then the corresponding concentration ratio may be defined

$$R_{\text{i.v.}} = (C_P/C_B)_{\text{i.v.}} \tag{5}$$

The pharmacokinetic advantage R_d is defined as the ratio:

$$R_d = R_{\text{i.p.}}/R_{\text{i.v.}} \tag{6}$$

Conceptually, R_d expresses the relative advantage that may be achieved by administration of a drug directly into the peritoneal cavity compared with i.v. administration. It has been shown [30] that the pharmacokinetic advantage may be expressed as a remarkably simple equation if there is no elimination of the drug from the peritoneal region:

$$R_d = 1 + CL_{BC}/MTAC \tag{7}$$

where CL_{BC} = total body clearance (cm^3/min). The same equation may be used for drug that is not administered by continuous infusion to steady state if the exposure terms are defined as the areas under the peritoneal and plasma concentration curves (AUC_P and AUC_B) following any schedule of administration if the system is linear in the sense that none of the relevant parameters change with drug concentration or time.

Equation 7 indicates a large pharmacokinetic advantage for most hydrophilic drugs administered to the peritoneal cavity. For example, a typical antibiotic would be expected to have a $MTAC$ of the order of 10 mL/min (Fig. 30.3). If the drug is cleared from the body by glomerular filtration at the rate of inulin, 125 mL/min [86], then the expected value of R_d is approximately 14.

Many drugs are eliminated by tissues within the peritoneal cavity, particularly the liver. This provides a first-pass effect, which has the effect of increasing the natural pharmacokinetic advantage given by Eq. 7. The regional advantage expected in the presence of some extraction of the drug by liver may be obtained from Dedrick [23]:

$$R_{i.p.} = \frac{1 + \frac{CL_{BC}}{MTAC}}{1 - fE} \tag{8}$$

where f = the fraction of the absorbed drug that enters the liver through the portal system or by direct absorption into its surface, and E = the fraction of that drug which is removed by the liver on a single pass. The quantity $(1 - fE)$ is the fraction of the absorbed drug that reaches the systemic circulation. If this fraction is small, then the natural advantage to regional administration can be considerably enhanced.

We do not have adequate information on the value of f. It is generally thought that small molecular weight compounds are absorbed primarily through the portal system [87]; however, there is evidence that some significant fraction of the absorbed drug can bypass the liver [12]. In the Speyer study, concentrations of 5-fluorouracil were observed to be higher in a peripheral artery than in the hepatic vein in three of four patients. Calculation of f was not reliable because analysis of the data depended upon knowledge of the blood flows in the portal vein and drug metabolism by gastrointestinal tissues, and these were not measured. The fact that about 15–20% of the peritoneal surface area covers tissues which are not portal to the liver is consistent with the transport observations.

Application of Model to the Pharmacokinetic Advantage

Antibiotics: Vancomycin

Intraperitoneal antibiotic therapy is used to treat localized peritonitis. The goal of such therapy is the same as that of antineoplastic agents: to maximize the concentration in the cavity in order to target the superficial tissues in the peritoneal cavity. Since the subject of i.p. antibiotic therapy has been covered thoroughly in another chapter of this text, we will illustrate the general approach to calculation of the regional pharmacokinetic advantage by application of the theory to vancomycin, a drug that is currently one of the recommended therapies for i.p. infections due to gram-positive organisms, which are resistant to cephalosporins and penicillins [9].

Vancomycin has a molecular weight of 1,500; 55% of the drug is bound to serum protein [88–90]. Its volume of distribution is variable and is cited over a range of 0.64 L/kg in normal young humans [90] to 0.93 L/kg in the elderly [88, 90]. Patients with renal failure (creatinine clearance less than 10 mL/min) have volumes of distribution averaging 0.9 L/kg [89]. The serum half-life of vancomycin is typically 6 h. However, since 90% of the injected dose is excreted by the kidney [91, 92], the normal half-life of 6 h becomes markedly prolonged in renal failure. Clearance of the drug in a normal (70 kg) patient is 100–140 mL/min. In the patient with renal failure the clearance is correlated with iothalamate, a marker for glomerular filtration rate [91]. Typical clearance rates for patients with creatinine clearance less than 10 mL/min average approximately 5 mL/min [89, 93].

The overall MTAC estimated from Fig. 30.3 is 4.0 mL/min. For the purpose of illustration, let us assume that the overall clearance from the body of our patient on peritoneal dialysis is 5 mL/min and that the drug is given by continuous infusion. Under these circumstances, the relative advantage of i.p. administration relative to i.v. administration is calculated from Eq. 11 modified to account for protein binding: $R_d = 1 + 5/(4.0 \times 0.45) = 3.8$.

Because of the long half-life and the toxicity of high serum levels that might result if continuous infusion were performed [88], the drug is usually given in either a single i.p. dialysate dwell every 24 h or as an i.v. infusion approximately once a week. Bunke et al. [94] studied vancomycin pharmacokinetics by dosing patients with either

10 mg/kg i.v. in a saline solution over 30 min or 10 mg/kg diluted in 2 L of 1.5% dextrose dialysate, which was allowed to dwell over 4 h. By computing the AUC_P/AUC_B for i.p. delivery during the first 24 h, the regional advantage ($R_{i.p.}$) is 429/109 = 3.9. Repeating the same for i.v. delivery, the AUC_P/AUC_B ($R_{i.v.}$) is 78.4/297 = 0.26. The pharmacokinetic advantage would then be $R_{i.p}/R_{i.v.}$ = 3.9/0.26 = 15. This provides a strong theoretical and experimental argument for i.p. vancomycin in appropriate cases of peritonitis.

Intraperitoneal Insulin

Human insulin is a small protein with a molecular weight of 5,808, which is secreted by the beta cells of the pancreatic islets of Langerhans in response to a glucose load in the plasma [50]. The secretion occurs directly into blood which circulates via the portal vein to the liver. The bulk of the hormone in the blood is in the unbound form [95]. Extraction of the hormone by the liver is receptor-mediated, saturable, and typically amounts to 40–60% of the drug delivered in the portal system [96]. After entering the general circulation, insulin distributes to the entire extracellular space [97]. In particular, insulin circulates to the kidney and muscle, which, aside from the liver, are its other major targets. Under normal conditions there is a portal-to-peripheral insulin concentration gradient, with the highest concentrations in the liver [95]. In an effort to control diabetic hyperglycemia in a more physiological way, replacement insulin is increasingly being administered intraperitoneally in order to mimic the normal physiology [96, 97].

Insulin is often administered dissolved in the dialysate to diabetic patients who suffer from ESRD and are treated with CAPD [98]. This results in the simultaneous transfer of insulin and dextrose from the cavity into the body and generally results in stable levels of blood glucose and insulin, which are below the corresponding levels with subcutaneous insulin [99]. Because of the extensive extraction by the liver, Eq. 8 must be used in order to predict the regional advantage of i.p. insulin therapy. Rubin [3] has shown that the transport properties of insulin (mass-transfer-area coefficient or $MTAC$ = 2.9 mL/min) are nearly identical to those of inulin ($MTAC$ = 3.3 mL/min). Because of similar molecular size, parameters for inulin are typically substituted for those of insulin. Transport is probably highest across the surfaces of the liver and of other viscera because their combined surface area makes up 60–65% of the total peritoneal area. In Eq. 8, assume that f = 0.9 and E = 0.5 and the $MTAC$ from Fig. 30.3 is 2.3 mL/min. While the normal total body clearance of insulin is typically 650–750 mL/min (referenced to 1.73 m^2), the clearance of [^{125}I] insulin is approximately half or 350 mL/min in chronic renal failure [100, 101]. The regional advantage can be calculated from Eq. 12: R_R = [1 + 350/2.3]/(1 − 0.9(0.5)) = 278. The measured ratio of intraperitoneally administered [^{125}I]insulin (AUC_P/AUC_B) was approximately 500 in dogs [98] and the value was 200–300 in humans [102].

Recent efforts in insulin replacement therapy for patients who suffer from diabetes mellitus, but who are not on dialysis, have tested i.p. administration as a more physiological method of drug delivery [97]. In a study that compared free insulin peaks after i.m., s.c, and i.p. injections, i.p. insulin produced serum insulin peaks at 15 min, while i.m. and s.c. insulin resulted in a much slower increase with peaks at 60 and 90 min, respectively [103]. The rapid rise in serum insulin, produced by i.p. administration, followed by a gradual fall in concentration, more closely mimics the true pancreas. The same study demonstrated that insulin delivered to the upper part of the peritoneal cavity was more quickly absorbed than insulin introduced into the lower part of the cavity. This is probably due to the rapid transfer into tissues of the gastrointestinal tract and direct diffusion into the liver. Delivery into the cavity by a pump has also led to more consistent serum levels than with administration into s.c. tissue, which produces variability in absorption rates [104].

In contrast to the relatively steady delivery of i.p. insulin in CAPD, this i.p. delivery therapy is typically given episodically in small volumes in the upper part of the cavity. The ratio of portal to systemic venous levels of insulin (AUC_{portal}/AUC_B) can give us a rough estimate of the utility of the delivery technique. It should be pointed out that the concentration in the portal vein probably reflects only a portion of the insulin delivered to the liver, since direct absorption across the surface of the liver is known to occur [105]. Selam et al. [106] have demonstrated in dogs that the ratio of i.p. insulin delivery to the portal vein over the amount appearing in the plasma is 17. This supports the concept of i.p. delivery of insulin in order to re-establish a more normal portal-to-peripheral insulin concentration gradient.

Antineoplastic Agents

The pharmacokinetic rationale for the i.p. administration of drugs in the treatment of microscopic residual ovarian cancer was described in 1978 [76]. The procedure has been the subject of numerous preclinical and clinical studies

during subsequent years, and these have been reviewed periodically [27, 28, 107]. The pharmacokinetic theory has been consistently validated, and there is clear evidence of response in terms of surgically staged complete remissions in a number of studies. Markman et al. [21] reviewed several of these and concluded that there may be an advantage to regional drug delivery of cisplatin-based therapy for small-volume refractory residual ovarian cancer. Subsequently, Markman et al. [108] concluded that attainment of a surgically staged complete remission may have a favorable impact on survival. Recently, Muggia et al. [25] demonstrated substantial activity with i.p. floxuridine (FUDR). Due to positive results of recent clinical trials[15, 22, 29, 109], i.p. drug therapy in the management of abdominal cancer has been designated as the standard of care by the National Cancer Institute [110].

Some of these principles are illustrated by a discussion of two specific drugs: *cis*-diamminedichloroplatinum(ii) (cisplatin) and 5-fluorouracil (5-FU). At issue are both the pharmacology of intracavitary administration and the depth of penetration of drug into both normal and neoplastic tissues.

Cisplatin

Cisplatin is among the most active agents used in the treatment of ovarian cancer. Its pharmacokinetics have been studied extensively, and a physiological model has been developed and applied to several species [111–113]. Briefly, the drug reacts with both small and large molecular weight nucleophiles in plasma and tissue compartments. The tissue-specific rate constants vary among the tissues but are relatively constant across species. Release of (presumably inactive) platinum from macromolecules is dominated by their catabolism.

Goel et al. [26] studied the i.p. administration of cisplatin in combination with etoposide, and examined the effect of concurrent i.v. administration of sodium thiosulphate to protect the kidney against platinum toxicity. They administered the drug combination in 2 L of normal saline and observed a cisplatin clearance from the peritoneal cavity of 15 mL/min and a clearance from the plasma of 329 mL/min. These clearances resulted in a regional advantage (AUC_P/AUC_B) of 26 in those patients who did not receive sodium thiosulphate. This advantage is similar to the value of 16 obtained by Piccart et al. [114] for cisplatin administered in combination with melphalan.

Los et al. [115] conducted pharmacokinetic studies of cisplatin in rats bearing CC531 colonic adenocarcinoma on serosal surfaces of the peritoneal cavity in order to determine the effect of route of administration on tumor and normal tissue levels of platinum. The AUC_B was approximately the same following both i.v. and i.p. administration, while the regional advantage was 7.6 based on ultrafiltered plasma and peritoneal fluid. Clearance from the peritoneal cavity may be calculated from their data to be 0.42 mL/min for a 200 g rat. The rat clearance is thus predictive of the human values on the basis of body weight to the 2/3 power in general agreement with the allometric variation in Fig. 30.4.

Average tumor levels of platinum in the i.p. group were twice those in the i.v. group; however, the excess platinum was confined to the periphery of the tumour. Measurements of platinum concentrations by proton-induced X-ray emission (PIXE) showed substantially higher levels in the outer 1.0 mm of the tumor; concentrations at 1.5 and 2.2 mm from the surface were independent of route of administration of the drug. This limited penetration is consistent with theoretical calculations for hexose [116] and experimental data for [^{14}C]EDTA [117] in normal tissues. It is instructive to apply a penetration model to cisplatin. As a rough approximation, let us assume that the diffusivity in tissue, D, is 1.9×10^{-6}cm^2/s based on transport in brain [118]; that the capillary permeability-area density (pa) product is of the order of 1.4×10^{-6} s^{-1} based on hexose in jejunum; and that the tissue-specific reaction rate, k, is 8×10^{-5} s^{-1} based on muscle [112]. Then the nominal diffusion distance $[D/(pa + k)]^{1/2}$ is 0.4 mm, which would imply that 9/10 of the gradient would be confined to the first millimeter from the surface of the tissue. While these calculations are provided for illustrative purposes, and are very approximate, they are almost certainly much better that order-of-magnitude. They support the idea that direct diffusion of cisplatin into tissue is very limited in extent.

The above reaction ($k = 8 \times 10^{-5}$ s^{-1}) and permeability (1.4×10^{-3} s^{-1}) parameters predict that $[1.4 \times 10^{-5}/(1.4 \times 10^{-3} + 8 \times 10^{-5})](100) = 95\%$ of the drug would be expected to be absorbed into the systemic circulation. This large bioavailability is consistent with the observations of Los et al. [115] in the tumor-bearing rat and of Pretorius et al. [119] in the dog, as well as with considerable human experience.

5-Fluorouracil (5-FU)

As discussed by Chabner [120], phosphorylation of 5-FU to nucleotide analogues appears necessary for its subsequent biological effects. Elimination from the body is primarily by metabolism believed to require reduction of the pyrimidine ring by dihydrouracil dehydrogenase. This enzyme is present in both the liver and other tissues such as the gastrointestinal mucosa. 5-FU exhibits strongly nonlinear elimination in human subjects with a half-saturating concentration of 15 μM as reviewed and discussed in the development of a physiological pharmacokinetic model [121].

Further, the observation of total-body clearances at low infusion rates that considerably exceed expected hepatic blood flow suggests the presence of extensive extrahepatic metabolism.

5-FU has pharmacological properties that commended it to i.p. trials in the treatment of intra-abdominal cancer. It is a hydrophilic drug with a molecular weight of 130 Da, which would be expected to have a relatively slow clearance from the peritoneal cavity (Fig. 30.3) and a total-body clearance ranging from 0.94 L/min at an infusion rate of 134 mg/kg/day to as high as 4–7 L/min at infusion rates of 10–30 mg/kg/day [121]. In addition to the high ratio of CL_{BC} to predicted MTAC, significant removal of the drug by peritoneal tissues would be expected to further limit systemic exposure.

The prediction of a high regional advantage has been shown in a number of clinical trials. Values of the AUC ratio between peritoneal cavity and plasma have been reported to be strongly dose-dependent, ranging from 124 at a dose of 3.5 mmol/L to 461 at a dose of 2.0 mM [19]. These are in general agreement with the observations of Speyer et al. [11], who observed peritoneal-to-plasma concentration ratios of 298 at 4 h and of Sugarbaker et al. [109] who reported a mean AUC ratio of 200 in patients administered 5-FU in the immediate postoperative period. Clearance from the peritoneal cavity has been in good agreement with the predictions from Fig. 30.3: 14 mL/min [11] and 24 mL/min [19]. Nonlinearity in systemic exposure deriving from the saturable metabolism (and possible saturable first-pass effect) of the agent was associated with an extraordinarily steep dose-response curve [11].

There has been considerable interest in the detailed mechanism of absorption of 5-FU from the peritoneal cavity because of the possibility of using this route as a way to perfuse the liver through the portal vein. Speyer et al. [11] placed catheters in the portal vein, hepatic vein, peripheral artery and peripheral vein of human patients. The hepatic extraction was calculated to decrease slightly from about 0.7 to 0.6 from the first to the seventh exchange. The estimated value of the fraction, f, of the absorbed drug entering the portal system was strongly dependent on assumptions relating to the blood flow rate in the portal vein and metabolism by tissues draining into the portal system, neither of which was directly assessed. Estimated values of f ranged from 0.3 to 1 depending on the assumptions made. There was direct evidence of drug bypassing the portal system in three of the four patients in whom the AUC in the peripheral artery actually exceeded the AUC in the hepatic vein. In studies in rats, Archer et al. [122] observed that systemic 5-FU levels were significantly lower during mesenteric vein infusion (0.9 ± 0.2 μM) compared with i.p. infusion at the same rate (2.1 ± 0.3 μM). Indirect evidence of a pharmacological first-pass effect is provided by the observations of Gianola et al. [123], who were able to administer a mean of 1.5 g per treatment cycle intraperitoneally but only 1.0 g intravenously; the i.p. route was actually accompanied by less hematological toxicity.

Approaches to Enhance Contact Area and Residence Time Intraperitoneally Administered Drugs

Drug delivery to metastatic cancer in the peritoneal cavity requires drug exposure and therefore is vitally dependent on sufficient contact between the therapeutic solution and the targeted tumor nodule(s). An approach to improve the contact area is to use a surface-active agent. In experiments with animals, diacetyl-sodium sulfosuccinate (DSS) has been shown to increase the surface contact area and to proportionally increase the rate of mass transfer into the local tissues [37, 70, 124]. More rapid uptake of the drug would result in a dissipation of the drug concentration from the fluid; this problem could be solved with the use of an automated exchange device such as a peritoneal dialysis machine, programmed to deliver periodic infusions over time of given concentration. Although DSS is used as an oral stool softener (docusate sodium), it unfortunately is quite toxic if administered i.p.; exposure of fluid containing surfactant to a larger proportion of the peritoneal surface area also accelerated the loss of protein and the dissipation of the drug concentration in the therapeutic solution [70].

In the perioperative setting, drug delivery can be enhanced considerably. Two catheters can be placed in the peritoneal cavity: one catheter for drug input and the other catheter for removal of solution. Solutions warmed to temperatures greater than body temperature (approximately 41°C) may be infused rapidly into the peritoneal cavity and withdrawn in the second catheter. This technique will set up higher concentrations if solution is fed from a large reservoir so that the loss of drug is relatively small. Additionally, with heating of the drug, causing vasodilation in the vessels, there is likely an increase in penetration into both normal tissue and neoplastic tissue [79–81, 125, 126]. This technique may help to solve the problem of residence time as well. If a greater portion of the peritoneal surface area is covered by the solution and the concentration of the drug is maintained constant, then the area into the curve for the surface contact concentration should be maximized. This will be restricted to perioperative patients, and the side effects of these drugs on normal peritoneum have not been studied.

Intraperitoneally Administered Drug Penetration in Neoplasms

Normal Versus Neoplastic Barriers in the Peritoneal Cavity

Penetration of 5-FU into tissues surrounding the peritoneal cavity has not been studied experimentally. Collins et al. [127] observed a strongly concentration-dependent rate of 5-FU disappearance from the peritoneal cavity of the rat. The peritoneal clearance increased from 0.20 mL/min, consistent with its molecular weight, to 10 times that value as the peritoneal concentration was decreased from 10 mM to 20 μM. This was explained by assuming that the drug is metabolized in tissues adjacent to the peritoneal cavity. A one-dimensional diffusion model with saturable intratissue metabolism (V_{max} = 36 nmol/min/g, K_M = 5 μM) simulated the peritoneal concentrations reasonably well. The model predicted that the concentration in the tissue would be 10% of its value at the tissue surface at a depth of 0.6 mm following a 12-mM dose; the corresponding 10% level would be reached at only 0.13 mm following a 24-μM dose. Observations that the toxicity profile associated with i.p. administration is similar to that observed following i.v. administration [12, 123] seem to confirm limited tissue penetration. If the drug reached the gastrointestinal crypt cells in high concentration, one would expect substantial toxicity there.

Predicting the concentration of the drug at the surface may or may not guarantee penetration of the drug into the tumor to the rapidly dividing tumor cells, which are the real target. The compartmental model concept lumps all of the potential barriers to the solute into one entity and does not differentiate between the variety of tissues, which may have different areas of contact and which may experience different transport forces. While Eq. 1 in conjunction with Eq. 2 permits calculation of the pharmacokinetic advantage, the model does not tell us anything about the specific penetration into the tissue. It merely describes the transfer between the two compartments. Illustrated in Fig. 30.5 is the distributed model concept [128], in which an idealized tissue space is modeled as a peritoneum overlying a tissue containing parenchymal cells and blood vessels surrounded by an interstitium; mathematical details of this theory are contained in previous publications [116, 128–130] and are beyond the scope of this chapter. Because intraperitoneal therapy involves the treatment of normal tissue as well as neoplastic tissue, it is important to differentiate between the properties of both of these. Figure 30.5 displays elements of the normal peritoneum with a tumor implant, which has destroyed the peritoneum and is growing within the tissue. The normal peritoneal barrier is made up of peritoneum, interstitial matrix, and the blood capillary wall. Lymphatic vessels are also located between normal tissue planes within

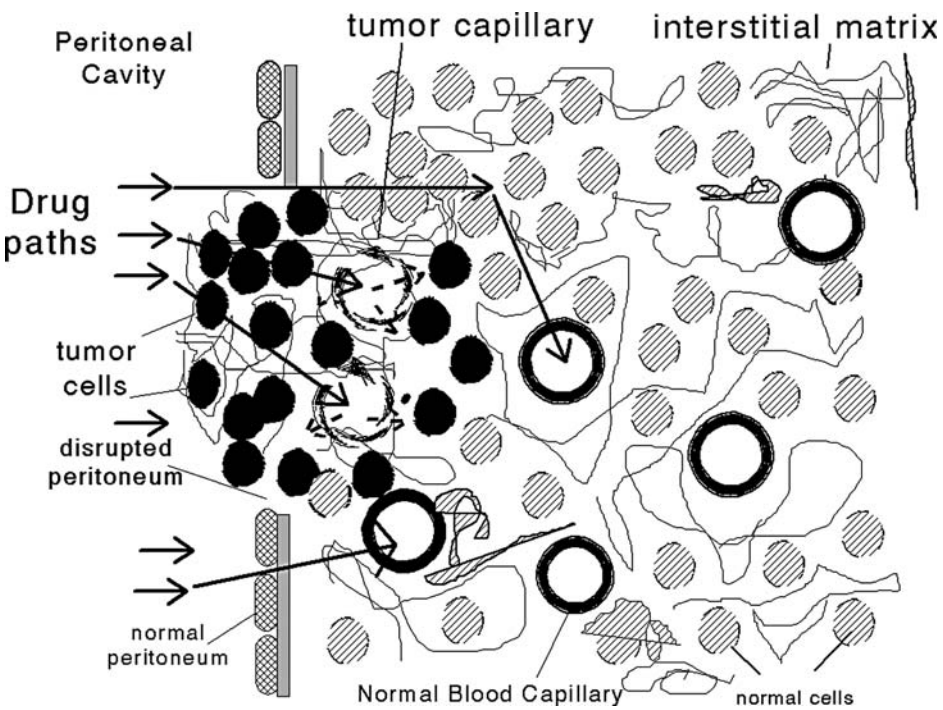

Fig. 30.5 Distributed model concept of metastatic cancer and potential barriers to i.p. therapy. Solid circles represent the tumor metastases, which have invaded and destroyed the mesothelium in its vicinity. Tumor capillaries (discontinuous circles) are typically more permeable than the normal microcirculation and set up high interstitial flows and pressures. The tumor microenvironment (interstitium between cells) is often markedly expanded compared to that of normal tissue. See text for details

smooth muscle or in the diaphragm. The differences between tumor and normal tissue include: lack of a mesothelial layer over the tumor, a very altered interstitium, and a hyperpermeable microcirculation. The following paragraphs will discuss the transport barrier for the normal peritoneum and the abnormalities of neoplastic tissue.

Anatomic Peritoneum

While the peritoneal barrier is often called the "peritoneal membrane," the actual anatomic peritoneum, made up of a layer of mesothelial cells and several layers of connective tissue [131], is not a significant barrier to molecules up to a molecular weight of 160,000 Da. Studies in rodents and dialysis patients have shown that protein leaves the cavity rates of approximately 10 times the rate at which it appears in blood [132–136]. The only route of transfer of protein in the cavity back to the central circulation is via the lymphatics [34, 137, 138]. There must be some other pathway for disappearance of this protein. In experiments with rodents, it has been shown that, as protein transports across the peritoneum, there is some adsorption [39] to the peritoneal cells but most of the protein deposition is into the subperitoneum. Further experiments demonstrated that removal of the peritoneum does not eliminate the dialytic properties of the peritoneal barrier [139]. Recent studies in patients undergoing partial or total peritonectomy for treatment of peritoneal carcinomatosis confirm the findings in rodents; the clearance of mitomycin C from the peritoneal cavity was not significantly affected by an extensive peritoneal resection [140].

Although proteins appear to easily pass the mesothelium into the subperitoneum, viral vectors containing gene products are taken up directly into mesothelial cells with little penetration beyond this single cell layer. Adenoviruses that code for the reporter gene β-galactosidase have been shown to be quantitatively taken up in mesothelium and not to penetrate into underlying tissues unless there is a break in the mesothelium [141–148].

The peritoneum at the site of tumor implantation will likely be destroyed in most cases of neoplastic cellular infiltration of the peritoneum (see Fig. 30.5). The loss of the mesothelium promotes adhesions, presents problems to the maintenance of the smoothly gliding peritoneal surface of the gut, and decreases the function of the immune system. Without the mesothelium, adhesions form between the visceral and parietal surfaces, and the fluid distribution may become markedly abnormal, which may preclude intracavitary therapy [149]. However, treatment with viral vectors containing anti-sense RNA or other gene products, which might not be capable of passing through the normal mesothelium, have the possibility to penetrate into the tumor from the peritoneal cavity [147].

In summary, the normal anatomic peritoneum is not a significant barrier to small solutes or to macromolecules, unless there exists a mechanism of uptake by the mesothelial cells, as in the case of viral vectors. The normal mesothelium may be destroyed by a metastatic tumor, which opens this abnormal tissue to penetration of viral vectors.

Interstitium or Tumor Microenvironment

Interstitium or the so-called "microenvironment" is made up of collagen fibers linked through adhesion molecules such as β-1 integrins to fibroblasts, parenchymal cells, and other interstitial cells [150, 151]. Hyaluronan molecules, which vary from 50,000 Da to 40 million, wrap around the collagen fibers and are likely attached to them at some link point. To the hyaluronan are attached large molecules called proteoglycans that also interact with the surrounding cells [152, 153]. Hyaluronan molecules are highly negatively charged and imbibe large amounts of water and restrict the passage of negatively charged proteins [154]. Proteins such as immunoglobulins are typically restricted to about 50% of the interstitial space [155, 156]. Thus, the interstitial space of normal muscle, which is anywhere from 12 to 20% of the total tissue volume, restricts proteins to 6 to 10% of the tissue. The transport of large solutes such as immunoglobulin G (150 kDa) or adenovirus (900 kDa) will be highly retarded by the microenvironment, as illustrated in Fig. 30.6, which compares the concentration profiles of small solutes and macromolecules in normal and neoplastic tissue.

Alterations in the interstitial pressure can change the relative tissue interstitial water space and the proportion of the tissue available to the solute. It has been shown in animal experiments that the abdominal wall interstitium will double when the intraperitoneal pressure is increased from 0 to 4 mm Hg [157, 158]. This will markedly enhance the transport of both small and large solutes through this space. The hydraulic conductivity or water permeability of the tissue also increases with increasing intraperitoneal pressure and washout of hyaluronan from the tissue interstitium [159]. Since the surface contact area is maximized with increasing peritoneal volumes [72, 82], attempts to increase the contact area will increase the pressure as well. The i.p. pressure varies directly with. the i.p. volume [160, 161] for normal dialysis patients. The effect of pressure is greatest in the abdominal wall where a nearly linear pressure gradient from the inside of the peritoneal cavity to the outside has been measured in the rat [162]; these profiles may be quite different from those in tumors [163] or in the human abdominal wall. Patients with adhesions or extensive surgical resection may have restricted volumes and very different pressure-volume characteristics, with increased pressures at lower volumes than those of dialysis patients. In summary, large volumes in the cavity increase the intraperitoneal pressure and expand the

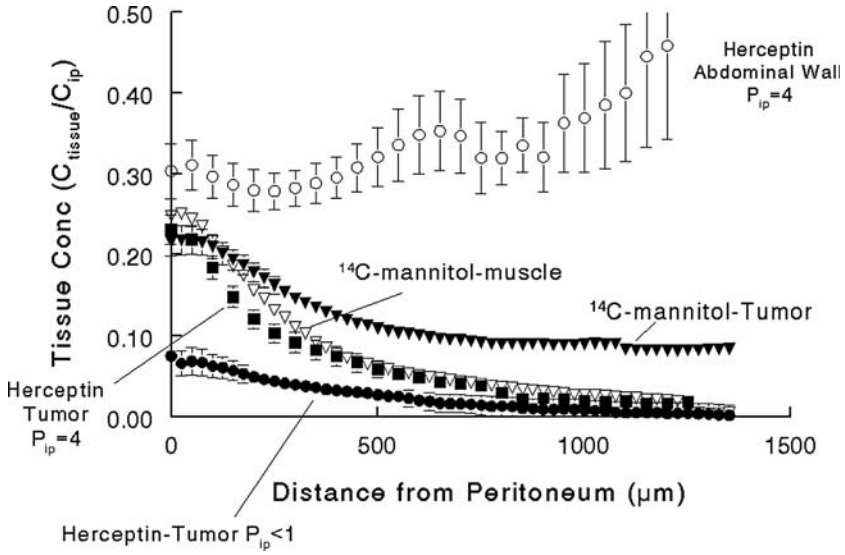

Fig. 30.6 Comparison of penetration of mannitol or Herceptin (IgG monoclonal, Her2/neu) into normal tissue (open symbols) or IP SKOV3 xenograft (closed symbols) of the rat after 3 h of treatment with a large i.p. volume. Mean ± SE concentrations versus distance in microns from the peritoneal surface. Replotted from [163, 169, 194]

interstitial space and, in turn, augment the space within the tissue to which both small and large solutes distribute. Antineoplastic agents will transport at faster rates through normal tissue due to increases in both diffusion and convection [129, 157, 159, 164–166].

There exist remarkable differences between the tumor microenvironment and that of normal interstitium. Interstitial pressures in normal tissue are in the range of −2 to 0 mm Hg [167, 168]. This allows convection due to the hydrostatic pressure gradient from the solution in the cavity (3–10 mm Hg) into the tissue. Unfortunately, several investigators have observed high interstitial pressures up to 45 mm Hg in neoplastic tissue [163, 169–172]. To deliver macromolecules by convection from the cavity into these tumors, the solution would have to attain a pressure greater than that of the tumor. The upper limit of pressure tolerated by an ambulatory patient is approximately 8–10 mm Hg in the peritoneal cavity [62, 163] and may limit the penetration of large solutes that depend on convection or solvent drag, if the tumor interstitium has a pressure higher than the i.p. pressure. In addition, steady i.p. pressures of >15 mm Hg in a closed cavity may suppress the portal circulation [62]. Pressures of >20 mm Hg may prevent the descent of the diaphragm [62] and compromise respiration. Therefore, an unanesthetized ambulatory patient will likely be unable to tolerate therapy, which depends on large volumes (>3–4 L) to produce high i.p. pressure. If tumor interstitial pressures are higher than those that can be attained, therapy with macromolecule may be precluded. Anesthetized patients, who receive mechanical ventilation, may be able to tolerate higher levels of i.p. pressure, but the mesenteric circulation supplying the gut should be carefully monitored.

Studies of tumor interstitium show that the space between the cells is often markedly expanded in comparison to normal tissue [173]. A recent study in human ovarian carcinoma xenografts demonstrated an interstitial water space of 2–3 times that of normal muscle [169]. Gullino and colleagues have shown similar results in several tumors [173]. Thus, the high interstitial pressure results in an expanded interstitium, which would typically result in higher rates of diffusion and convection in normal tissue. However, the high interstitial pressure and intrinsic properties of the tumor interstitium resist any transfer of large molecules into the tumor [170, 174–177]. On the other hand, smaller substances (molecular weight < 500 daltons) will diffuse into the tumor parenchyma in a fashion similar to normal tissue [117, 169].

Microcirculation

Normal blood capillary endothelia are lined with a glycocalyx, which has been demonstrated to provide the endothelium with its barrier characteristics [178–181]. In portions of the interendothelial cleft, it is theorized that the glycocalyx is quite dense and only small molecules up to the size of insulin (~5,500 Da) will typically pass through while in other areas a small number of gaps will have a less dense glycocalyx, which will permit protein leakage [166]. This provides the size selective nature of the normal peritoneal barrier. However, inflammation or drugs such as adenosine [182] cause the elimination or degradation of the glycocalyx and an increase the capillary permeability; the vessels of the

normal peritoneum are likely affected during inflammation due to invasion by metastatic carcinoma [183]. Capillary permeability is markedly altered in neoplastic tissue, with typically a high permeability but a variable microvascular density [184, 185]. Although detailed studies have not been carried out, all indications are that these highly permeable capillaries may be responsible for the rapid clearance of drugs into portions of the tumor from the systemic circulation [186]. While this can be an advantage in treatment of these tumors, the high pressures in the interstitium may actually result in difficulty in drug penetration [185, 187]. The nature of angiogenic vessels is under scrutiny; these may not have the glycocalyx that lines the normal endothelium and provides much of the barrier to solute transfer [184, 186–188]. Thus, many of the characteristics of these new vessels may be completely different from those of normal vasculature. In addition, the actual distribution of vessels is very irregular. In small (<1 cm diameter) ovarian xenografts, the vessels are located in the periphery of the tumor, which is expanding into the normal tissue [169]. The central part of the tumor may actually be necrotic and have no vasculature at all. Penetration to nonvascularized portions of the tumor is one of the problems of i.v. or i.p. administration. Targeting the vasculature simultaneously with intraperitoneal therapy may be a method of accessing these portions of the tumor and solving this problem.

Lymph drainage from the cavity is chiefly through the subdiaphragmatic lymphatics [166]. In normal conditions, the relaxation of the diaphragm will open specialized "stomata," which accept proteins, cells, and solution from the peritoneal cavity into collecting lymphatics [32, 189]. The subsequent contraction of the diaphragm will close the stomata and propel the material into the parasternal lymphatics and ultimately into the right or left lymph duct. Approximately 70–80% of peritoneal lymph drainage occurs through this route [34]. Lymphatics from the viscera drain to the cisterna chyli at the base of the thoracic duct and ultimately into the left venous system [138].

With peritoneal carcinomatosis, the subdiaphragmatic lymphatics and the mesenteric lymphatics may be obstructed [190, 191]. The obstruction produces severe ascites because the normal flow of fluid and proteins from the viscera into the peritoneal cavity cannot be cleared properly [191]. In addition, the lymphatics provide a route of metastasis to the remainder of the body; including the periaortic and thoracic nodes [192]; often supradiaphragmatic nodes are overwhelmed with tumor cells; these same nodes then allow tumor cells to pass into the systemic circulation. However, if these pathways are still functional, intraperitoneal therapy directly targets these routes of metastasis and is a direct route to the systemic circulation for all agents, particularly those with molecular sizes greater than that of albumin.

Summary of Normal Versus Neoplastic Peritoneal Barrier

The anatomic peritoneum is not a barrier to most drugs, including immunoglobulins. The mesothelial layer may be absent in a tumor implant on the peritoneum and the vasculature and the microenvironment may be greatly altered. While viral vectors are totally absorbed in the normal mesothelium, its absence at a tumor surface may permit these very large particles (~900 kilodaltons) to pass into the first few cell layers of the tumor; however viral vectors will still have restricted movement in the tumor interstitium [177]. The interstitium is markedly expanded and theoretically should promote high rates of diffusion and convection [169, 177]. However, the high interstitial pressure and the tendency of flow from the center part of the tumor towards the periphery may cause a functional obstruction in the direction of the treatment drug originating from the peritoneum cavity [163, 170, 172, 193]. In addition, there appear to be structural differences in the collagen matrix of the tumor interstitium that prevent significant convection and diffusion of negatively charged, macromolecular agents [176, 177]. The tumor blood capillary and microcirculation are markedly abnormal in distribution and permeability characteristics [184, 185, 187]. Depending on the location and density of the tumor microvasculature, systemically administered drugs may rapidly distribute to perfused regions of the tumor but not reach poorly vascularized locations altogether. Multi-agent therapies that simultaneously attack the interstitium, vasculature, and the peritoneal side of the tumor will therefore likely be more effective in remitting peritoneal carcinomatosis.

Penetration of Small Molecules: Distributed Model Theory

The distributed model concept permits estimates of drug penetration. The theory for small solutes (≤1,000 Da), which depend almost exclusively on diffusion for transport through the tumor, is presented below. Application of the theory for macromolecules, which transport chiefly by convection, is complicated by a lack of transport parameters within the tumor parenchyma and the variability of the microcirculation and tumor microenvironment [130].

Transfer of small molecules from the peritoneal cavity can be viewed as a process of diffusion from the fluid in the cavity into the adjacent tissues followed by absorption from the tissue extracellular space into blood in the exchange vessels (Fig. 30.5). Convection generally does not play a quantitatively significant role for small solutes [194], and

lymphatic uptake is negligible compared with removal from the tissue by the flowing blood. The result is that a concentration profile is established within the tissue. At steady state the rate of diffusion down the profile at any location is exactly balanced by the combination of irreversible chemical reaction in the tissue and removal by flowing blood. For a nonreactive solute and a uniformly distributed capillary network, it is easily shown that the rate of uptake into blood perfusing the viscera may be calculated from the equation [116]:

$$S_{\mathrm{i}} = \sqrt{D_{\mathrm{i}}(p_{\mathrm{i}}a_{\mathrm{i}})}A_{\mathrm{i}}(C_{\mathrm{P}} - C_{\mathrm{B}}) \tag{9}$$

where S_{i} = net rate of uptake of the solute in tissue "i" (μg/min), D_{i} = the effective diffusivity of the solute in tissue "i" (cm^2/min), p_{i} = the intrinsic permeability of the blood capillaries in tissue "i" (cm/min), a_{i} = the capillary surface area per unit tissue volume ($\mathrm{cm}^2/\mathrm{cm}^3$), A_{i} = the superficial surface area of tissue "i"exposed to peritoneal fluid (cm^2), C = the free solute concentration (μg/cm^3), and the subscripts P and B refer to peritoneal fluid and blood, respectively (see Fig. 30.1). The effective diffusivity is equal to the diffusivity in the tissue interstitial space multiplied by the tissue fractional interstitial space, which is available to the solute.

A number of observations may be made about Eq. 9. First, the effective diffusivity, capillary permeability, and capillary surface area enter as their square root so that doubling of the capillary permeability, for example, would be expected to be associated with only a 41% increase in mass transfer ($2^{1/2} = 1.41$); second, the net transport rate is proportional to the superficial area of the tissue; and, third, the rate of transport is proportional to the difference in the free concentration of solute between the peritoneal fluid and blood.

Equation 9 serves as the basis for the definition of an equivalent MTAC of the tissue. If there were a thin membrane separating the peritoneal fluid from the blood, the rate of uptake would be given by

$$S_{\mathrm{i}} = MTAC_i(C_{\mathrm{P}} - C_{\mathrm{B}}) \tag{10}$$

Comparison of Eqs. 9 and 10 shows that the equivalent tissue permeability can be calculated from

$$MTAC_{\mathrm{i}} = A_i\sqrt{D_{\mathrm{i}}(p_{\mathrm{i}}a_{\mathrm{i}})} \tag{11}$$

Either Eq. 9 or 10 can be used to calculate the rate of absorption of a drug from the peritoneal cavity into the blood as they are exactly equivalent. The spatially distributed view of the tissue offers certain advantages because it provides some insight into the underlying transport mechanisms and how these might be altered by pathological processes or pharmacological manipulations. It also serves as a natural link to the very large body of literature on capillary physiology, and provides a natural framework to incorporate this into descriptions and predictions of peritoneal transport rates. Further, it explicitly predicts that a concentration profile extends a finite depth into the tissue, and tissue penetration is an important consideration if the goal of i.p. therapy is to treat disease in the tissue or disease of finite thickness such as peritoneal carcinomatosis on serosal surfaces. Explicitly, the concentration profile is given by:

$$\frac{C - C_{\mathrm{B}}}{C_{\mathrm{P}} - C_{\mathrm{B}}} = \exp -\sqrt{\frac{(p_{\mathrm{i}}a_{\mathrm{i}})}{D_{\mathrm{i}}}}x \tag{12}$$

where x is the distance from the serosal surface [116]. Equations similar to 9 and 10 can be written for as many types of peritoneal tissue as desirable. Since uptake rates into the various tissue types are parallel processes, they may be summed to provide an estimate of the overall drug transfer.

Concentration Profiles in Normal and Neoplastic Tissue

The profiles from i.p. administration of a small solute (mannitol, 180 Da) and the macromolecule Herceptin (IgG monoclonal antibody to the HER2/neu receptor, ~155,000 Da) are illustrated in Fig. 30.6 for normal abdominal wall (open symbols) and SKOV-3 xenografts (solid symbols) grown in the abdominal wall of athymic rats [163, 169, 177]. The mannitol has higher concentrations deeper within tumor tissue because the density of microvessels in normal tissue is higher than that of the xenograft [169]. On the other hand, despite an increase in i.p. hydrostatic pressure (P_{ip}), the macromolecular agent, Herceptin, is markedly retarded in the tumor in comparison to normal tissue [163]. While tumor interstitial pressure is a factor, the tumor interstitial collagen matrix is a major impediment to penetration of antibodies and other macromolecules [177].

Intraperitoneal Antibody Therapy and the Pharmacokinetic Advantage

An alternative to the typical antineoplastic agent in cancer therapy is the use of i.p.-administered monoclonal antibodies (Mab) in the treatment of intra-abdominal cancers. These antibodies, which are typically linked to some toxic agent, react specifically with antigens on the tumor cell and bind strongly, with subsequent killing of the cell [195]. As outlined in Dedrick and Flessner [196], the general equation for the calculation of the pharmacokinetic advantage is the same as that for small substances (see Eq. 7). The MTAC for immunoglobulin has been estimated from pore theory to be 0.05 mL/min [197]. The total-body clearance of IgG has been estimated to be 0.5–1.0 mL/min [196]. Inserting this into Eq. 7, one may calculate a R_d of 17–33. This suggests a considerable pharmacokinetic advantage in i.p. administration of monoclonal antibody.

The usefulness of this therapy must also be assessed in terms of the ultimate goal. Free ascites cells are readily accessible to MAbs [198]; in this case, the R_d would be the number calculated by Eq. 7. Unlike smaller molecules, however, large proteins do not penetrate tissues readily. Because of their large size (molecular radius = 52 Å), the effective diffusivity in tissue is on the order of 10^{-7}–10^{-9} cm^2/s [129, 199, 200]. Since this is two orders of magnitude less than the diffusivity of small molecules, the diffusive transport of macromolecules such as IgG within normal or neoplastic tissue is very slow. Recent mathematical analyses have also shown that MAbs with high affinity to their antigens are even more severely retarded by the "binding-site barrier" [176, 201–203]. The transport of these molecules is typically dominated by convection, both within the interstitial space [136, 204] and across capillary endothelium [205]. Tissue penetration studies of antibodies administered i.p. in animals [163, 164, 177, 200] have shown that most of the IgG is contained in the initial 300–400 μm of tissue during the first 3 h. These studies also demonstrated that diffusion probably plays only a minor role in the transport of the protein. Studies in tumor-bearing animals confirm these findings, and have not demonstrated large advantages of i.p. MAb administration over i.v. administration [198, 206]. This means that there may be limitations in the treatment of solid tumors and metastases with MAbs or other macromolecules.

Summary

Intraperitoneal chemotherapy should be considered as an alternative to i.v. therapy when the target is contained within the peritoneal cavity or within the adjacent tissue. A compartmental model has been used to formulate a mathematical scheme in order to evaluate the solute transport to specific tissue groups surrounding the cavity. Although the data to fully implement the model do not exist, a simplified version of the model with parameters derived from the literature can be used to solve for the steady-state concentrations in the peritoneal cavity and the plasma. The ratio of these two concentrations defines the regional advantage of i.p. therapy. Several applications of the theory are presented in order to illustrate the method in which i.p. therapy may be evaluated prior to use in patients. Application of the model to treatment of metastatic carcinoma is complicated by major differences in the targeted tissue properties. Recent animal data are discussed to illustrate the challenges of i.p. chemotherapy and immunotherapy for cancer.

Acknowledgment This work was supported by U.S. Public Health Service Grant RO1-DK-048479.

References

1. Cole W, Montgomery J. Intraperitoneal blood transfusion. Am J Dis Child 1929; 37: 497–510.
2. Clausen J. Studies on the effects of intraperitoneal blood transfusion. Acta Paediatr 1940; 27: 24–31.
3. Rubin J, Reed V, Adair C, Bower J, Klein E. Effect of intraperitoneal insulin on solute kinetics in CAPD: insulin kinetics in CAPD. Am J Med Sci 1986; 291: 81–87.
4. Catargi B. Current status and future of implantable insulin pumps for the treatment of diabetes. Expert Rev Med Devices 2004; 1: 181–185.
5. Gin H, Renard E, Melki V, EVADIAC Study Group. Combined improvements in implantable pump technology and insulin stability allow safe and effective long term intraperitoneal insulin delivery in type 1 diabetic patients: the EVADIAC experience. Diabetes Metab 2003; 29: 602–607.
6. Hovorka R. Continuous glucose monitoring and closed-loop systems. Diabet Med 2006; 23: 1–12.
7. Bargman J, Jones J, Petro J. The pharmacokinetics of intraperitoneal erythropoietin administered undiluted and diluted in dialysate. Perit Dial Int 1992; 12: 369–372.
8. Reddingius R, deBoer A, Schroder C, Willems J, Monnens L. Increase of the bioavailability of intraperitoneal erythropoietin in children on peritoneal dialysis by administration in small dialysis bags. Perit Dial Int 1997; 17: 467–470.

9. Piraino B, Bailie G, Bernardini J, Boeschoten E et al. Peritoneal dialysis-related infections recommendations: 2005 Update. Perit Dial Int 2005; 25: 107–131.
10. Jones RB, Myers CE, Guarino AM, Dedrick RL, Hubbard SM, DeVita VT. High volume intraperitoneal chemotherapy ('belly bath') for ovarian cancer. Cancer Chemother Pharmacol 1978; 1: 161.
11. Speyer JL, Collins JM, Dedrick RL, Brennan MF, Buckpitt AR, Londer H et al. Phase I and pharmacological studies of 5-fluorouracil administered intraperitoneally. Cancer Res 1980; 40: 567.
12. Speyer JL, Sugarbaker PH, Collins JM, Dedrick RL, Klecker RW, Myers CE. Portal levels and hepatic clearance of 5-fluorouracil after intraperitoneal administration in humans. Cancer Res 1981; 41: 1916.
13. Markman M. Intraperitoneal therapy of ovarian carcinoma. Semin Oncol 1998; 25: 356–360.
14. Markman M. Intraperitoneal chemotherapy in the management of colon cancer. Semin Oncol 1999; 26: 536–539.
15. Barakat RR, Sabbatini P, Bhaskaran D, Revzin M, Smith A, Venkatraman E et al. Intraperitoneal chemotherapy for ovarian carcinoma: results of long-term follow-up. J Clin Oncol 2002; 20: 694–698.
16. Ozols RF, Young RC, Speyer JL, Waltz M, Collins JM, Dedrick RL et al. Intraperitoneal (IP) adriamycin (ADR) in ovarian carcinoma (OC). Proc Am Soc Clin Oncol 1980; 21: 425.
17. Ozols RF, Young RC, Speyer JL. Phase I and pharmacological studies of adriamycin administered intraperitoneally to patients with ovarian cancer. Cancer Res 1982; 42: 4265–4269.
18. Gianni L, Jenkins J, Greene R, Lichter A, Myers C, Collins J. Pharmacokinetics of the hypoxic radiosensitizers misonidazole and demethylmisonidazole after intraperitoneal administration in humans. Cancer Res 1983; 43: 913–916.
19. Arbuck S, Trave F, Douglas H, Nava H, Zakrzewkski S, Rustum Y. Phase I and pharmacologic studies of intraperitoneal leucovorin and 5-fluorouracil in patients with advanced cancer. J Clin Oncol 1986; 4: 1510–1517.
20. Urba W, Clark J, Steis R. Intraperitoneal lymphokine-activated killer cell/interleukin-2 therapy in patients with intra-abdominal cancer: immunologic considerations. J Nat Cancer Inst 1989; 81: 602–611.
21. Markman M, Hakes T, Reichmann B, Hoskins W, Rubin S, Lewis J. Intraperitoneal versus intravenous cisplatin-based therapy in small-volume residual refractory ovarian cancer: evidence supporting an advantage for local drug delivery. Reg Cancer Treat 1990; 3: 10–12.
22. Alberts DS, Liu PY, Hannigan EV, O'Toole R, Williams SD, Young JA et al. Intraperitoneal cisplatin plus intravenous cyclophosphamide versus intravenous cisplatin plus intravenous cyclophosphamide for stage III ovarian cancer. N Engl J Med 1996; 335: 1950–1955.
23. Markman M, Rowinsky E, Hakes T. Phase I trial of intraperitoneal taxol: a Gynecologic Oncology Group Study. J Clin Oncol 1992; 10: 1485–1491.
24. Markman M, Brady M, Spirtos N, Hanjani P, Rubin S. Phase II trial of intraperitoneal paclitaxel in carcinoma of the ovary, tube, and peritoneum: a Gynecologic Oncology Group study. J Clin Oncol 1998; 16: 2620–2624.
25. Muggia F, Liu P, Alberts D. Intraperitoneal mitoxantrone or floxuridine: effects on time-to-failure and survival in patients with minimal residual ovarian cancer after second-look laparotomy – a randomized phase II study by the Southwest Oncology Group. Gynecol Oncol 1996; 61: 395–402.
26. Goel R, Cleary S, Horton C, Howell S. Effect sodium thiosulfate on the pharmacokinetics and toxicity of cisplatin. J Nat Cancer Inst 1989; 81: 1552–1560.
27. Markman M, Walker J. Intraperitoneal chemotherapy of ovarian cancer: a review, with a focus on practical aspects of treatment. J Clin Oncol 2006; 24: 988–993.
28. Ozols RF. Systemic therapy for ovarian cancer: current status and new treatments. Semin Oncol 2006; 33: S3–S11.
29. Yan T, Black D, Savady R, Sugarbaker P. Systematic review on the efficacy of cytoreductive surgery combined with perioperative intraperitoneal chemotherapy for peritoneal carcinomatosis from colorectal carcinoma. J Clin Oncol 2006; 24: 4011–4019.
30. Dedrick RL. Interspecies scaling of regional drug delivery. J Pharm Sci 1986; 75: 1047–1052.
31. Leak LV, Rahil K. Permeability of the diaphragmatic mesothelium: the ultrastructural basis for 'stomata'. Am J Anat 1978; 151: 557–594.
32. Bettendorf U. Lymph flow mechanism of the subperitoneal diaphragmatic lymphatics. Lymphology 1978; 11: 111–116.
33. Allen L. On the penetrability of the lymphatics of the diaphragm. Anat Rec 1956; 124: 639–658.
34. Yoffey JM, Courtice FC. Lymphatics, Lymph, and the Lymphomyeloid Complex. London, UK: Academic, 1970.
35. Flessner MF, Parker RJ, Sieber SM. Peritoneal lymphatic uptake of fibrinogen and erythrocytes in the rat. Am J Physiol 1983; 244: H89–H96.
36. Abernathy N, Chin W, Hay J, Rodela H, Oreopoulos D, Johnston M. Lymphatic drainage of the peritoneal cavity in sheep. Am J Physiol 1991; 260: F353–F358.
37. Flessner MF, Lofthouse J, Zakaria EL. Improving contact area between the peritoneum and intraperitoneal therapeutic solutions. J Am Soc Nephrol 2001; 12: 807–813.
38. Flessner MF, Dedrick RL, Reynolds JC. Bidirectional peritoneal transport of immunoglobulin in rats: compartmental kinetics. Am J Physiol 1992; 262: F275–F287.
39. Flessner MF, Schwab A. Pressure threshold for fluid loss from the peritoneal cavity. Am J Physiol 1996; 270: F377–F390.
40. Pearson CM. Blood Vessels and Lymphatics. New York: Academic, 1962.
41. Flessner MF, Dedrick RL, Schultz JS. A distributed model of peritoneal-plasma transport: analysis of experimental data in the rat. Am J Physiol 1985; 248: F413–F424.
42. Flessner MF, Dedrick RL, Schultz JS. Exchange of macromolecules between peritoneal cavity and plasma. Am J Physiol 1985; 248: H15–H25.
43. Rubin J, Clawson M, Planch A, Jones Q. Measurements of peritoneal surface area in man and rat. Am J Med Sci 1988; 295: 453–458.
44. Esperanca MJ, Collins DL. Peritoneal dialysis efficiency in relation to body weight. J Pediatr Surg 1966; 1: 162–169.
45. Ludwig J. Current Methods of Autopsy Practice. Philadelphia: WB Saunders, 1972.
46. Rhodin JA. Histology: A Text and Atlas. New York: Oxford Univ. Press, 1974.
47. DiFiore MSH. Atlas of Human Histology. Philadelphia: Lea & Febiger, 1974.

48. Rubin J, Jones Q, Planch A, Stanak K. Systems of membranes involved in peritoneal dialysis. J Lab Clin Med 1987; 110: 448–453.
49. Vetterlein F, Schmidt G. Functional capillary density in skeletal muscle during vasodilation induced by isoprenaline and muscular exercise. Microvasc Res 1980; 20: 156–164.
50. Guyton AC. Textbook of Medical Physiology. 6th ed. Philadelphia: WB Saunders, 1981.
51. Mapleson W. An electric analogue for uptake and exchange of inert gases and other agents. J Appl Physiol 1963; 18: 197–204.
52. Bonaccorsi A, Dejana E, Quintana A. Organ blood flow measured with microspheres in the unanesthetized rat: effects of three room temperatures. J Pharmacol Methods 1978; 1: 321–328.
53. Grim E. Handbook of Physiology. Washington: American Physiological Society, 1963.
54. Chou CC, Grassmick B. Motility and blood flow distribution within the wall of the gastrointestinal tract. Am J Physiol 1978; 235: H34–H39.
55. Crandall L, Barker S, Graham D. A study of the lymph flow from a patient with thoracic duct fistula. Gastroenterology 1943; 1: 1040.
56. Courtice FC, Simonds W, Steinbeck AW. Some investigations on lymph from a thoracic duct fistula in man. Aust J Exp Biol Med Sci 1951; 29: 201.
57. Morris B. The exchange of protein between the plasma and the liver and intestinal lymph. Q J Exp Physiol 1956; 41: 326–340.
58. O'Morchoe C, O'Morchoe D, Holmes M, Jarosz H. Flow of renal hilar lymph during volume expansion and saline diuresis. Lymphology 1978; 11: 27–31.
59. Shad H, Brechtelsbauer H. Thoracic duct lymph in conscious dog at rest and during changes of physical activity. Pfluegers Arch 1978; 367: 235–240.
60. Tran L, Rodela H, Abernathy N, Johnston M. Lymphatic drainage of hypertonic solution from peritoneal cavity of anesthetized and conscious sheep. J Appl Physiol 1993; 74: 859–867.
61. Aune S. Transperitoneal exchange: II. Peritoneal blood flow estimated by hydrogen gas clearance. Scand J Gastroenterol 1970; 5: 99.
62. Flessner MF. Transport of Water-Soluble Solutes Between the Peritoneal Cavity and Plasma in the Rat. Ann Arbor, MI: Univ. of Michigan, 1981.
63. Grzegorzewska AE, Moore HL, Nolph KD, Chen TW. Ultrafiltration and effective peritoneal blood flow during peritoneal dialysis in the rat. Kidney Int 1991; 39: 608–617.
64. Collins JM. Inert gas exchange of subcutaneous and intraperitoneal gas pockets in piglets. Respir Physiol 1981; 46: 391.
65. Kim M, Lofthouse J, Flessner MF. A method to test blood flow limitation of peritoneal-blood solute transport. J Am Soc Nephrol 1997; 8: 471–474.
66. Demissachew H, Lofthouse J, Flessner MF. Tissue sources and blood flow limitations of osmotic water transport across the peritoneum. J Am Soc Nephrol 1999; 10: 347–353.
67. Zakaria EL, Carlsson O, Rippe B. Limitation of small solute exchange across the visceral peritoneum: effects of vibration. Perit Dial Int 1997; 17 (1): 72–79.
68. Erb R, Greene J, Weller J. Peritoneal dialysis during hemorrhagic shock. J Appl Physiol 1967; 22: 131–135.
69. Rosengren BI, Rippe B. Blood flow limitation in vivo of small solute transfer during peritoneal dialysis in rats. J Am Soc Nephrol 2003; 14: 1599–2003.
70. Flessner MF, Lofthouse J, Williams A. Increasing peritoneal contact area during dialysis improves mass transfer. J Am Soc Nephrol 2001; 12: 2139–2145.
71. Chagnac A, Herskovitz P, Weinstein T, Elyashiv S, Hirsh J, Hamel I et al. The peritoneal membrane in peritoneal dialysis patients: estimation of its functional surface area by applying stereologic methods to computerized tomography scans. J Am Soc Nephrol 1999; 10: 342–346.
72. Chagnac A, Herskovitz P, Ori Y, Weinstein T, Hirsh J, Katz M et al. Effect of increased dialysate volume on peritoneal surface area among peritoneal dialysis patients. J Am Soc Nephrol 2002; 13: 2554–2559.
73. Hosie KB, Gilbert J, Kerr DJ, Brown C, Peers E. Fluid dynamics in man of an intraperitoneal drug delivery solution: 4% icodextrin. Drug Deliv 2001; 8: 9–12.
74. Hosie KB, Kerr DJ, Gilbert JA, Downes M, Lakin G, Pemberton G et al. A pilot study of adjuvant intraperitoneal 5-fluorouracil using 4% icodextrin as a novel carrier solution. Eur J Surg Oncol 2003; 29: 254–260.
75. Flessner MF. Small-solute transport across specific peritoneal tissue surfaces in the rat. J Am Soc Nephrol 1996; 7: 225–233.
76. Dedrick RL, Myers CE, Bungay PM, DeVita VT. Pharmacokinetic rationale for peritoneal drug administration in the treatment of ovarian cancer. Cancer Treat Rep 1978; 62: 1.
77. Krediet RT. Physiology of peritoneal solute transport and ultrafiltration. In: Gokal R, Khanna R, Krediet RT, Nolph K, editors. Textbook of Peritoneal Dialysis. Dordrecht: Kluwer Academic Publishers, 2000: 135–172.
78. Babb AL, Johansen PJ, Strand MJ, Tenckhoff H, Scribner BH. Bidirectional permeability of the human peritoneum to middle molecules. Proc Eur Dial Transplant Assoc 1973; 10: 247.
79. Jacquet P, Averbach A, Stephens A, Stuart O, Chang D, Sugarbaker P. Heated intraoperative intraperitoneal mitomycin C and early postoperative intraperitoneal 5-fluorouracil: pharmacokinetic studies. Oncology 1998; 55: 130–138.
80. Elias D, Bonnay M, Puizillou J, Antoun S, Demirdjian S, ElOtmany A et al. Heated intra-operative intraperitoneal oxaliplatin after complete resection of peritoneal carcinomatosis: pharmacokinetics and tissue distribution. Ann Oncol 2002; 13: 267–272.
81. Steller M, Egorin MJ, Trimble E, Bartlett D, Suhowski E, Alexander H et al. A pilot phase I trial of continuous hyperthermic peritoneal perfusion with high-dose carboplatin as primary treatment of patients with small-volume residual ovarian cancer. Cancer Chemother Pharmacol 1999; 43: 106–114.
82. Keshaviah P, Emerson PF, Vonesh EF, Brandes JC. Relationship between body size, fill volume, and mass transfer area coefficient in peritoneal dialysis. J Am Soc Nephrol 1994; 4: 1820–1826.
83. Torres IJ, Litterst CI, Guarino AM. Transport of model compounds across the peritoneal membrane in the rat. Pharmacology 1978; 17: 161–166.
84. Lewis C, Lawson N, Rankin E et al. Phase I and pharmacokinetic study of intraperitoneal thioTEPA in patients with ovarian cancer. Cancer Chemother Pharmacol 1990; 26: 283–287.

85. Wikes A, Howell S. Pharmacokinetics of hexamethylmelamine administered via the ip route in and oil emulsion vehicle. Cancer Treat Rep 1985; 69: 657–662.
86. Pitts R. Physiology of the Kidney and Body Fluids. Chicago: Year Book Medical Pub, 1963.
87. Lukas G, Brindle S, Greongard P. The route of absorption of intraperitoneally administered compounds. J Pharmacol Exp Ther 1971; 178: 562–566.
88. Moellering R. Pharmacokinetics of vancomycin. J Antimicrob Chemother 1984; 14 (suppl D): 43–52.
89. Matzke G, McGory R, Halstenson C, Keane W. Pharmacokinetics of vancomycin in patients with various degrees of renal function. Antimicrob Agents Chemother 1984; 25: 433–437.
90. Cutler N, Narang P, Lesko L, Ninos M, Power M. Vancomycin disposition: the importance of age. Clin Pharmacol Ther 1984; 36: 803–810.
91. Rotschafer J, Crossley K, Zaske D, Mead K, Sawcuk R, Solem L. Pharmacokinetics of vancomycin: observations in 28 patients and dosage recommendations. Antimicrob Agents Chemother 1982; 22: 391–394.
92. Nielsen H, Hansen H, Korsager B, Skov P. Renal Excretion of vancomycin in kidney disease. Acta Med Scand 1975; 197: 261–264.
93. Cunha B, Ristuccia A. Clinical usefulness of vancomycin. Clin Pharmacol 1983; 2: 417–424.
94. Bunke C, Aronoff G, Brier M, Sloan R, Luft F. Vancomycin kinetics during continuous ambulatory peritoneal dialysis. Clin Pharmacol Ther 1983; 34: 621–637.
95. Larner J. Insulin and oral hypoglycemic drugs and glucagon. In: Gilman A, Goodman L, Rail T, Murad F, editors. Goodman and Gilman's The Pharmacological Basis of Therapeutics. New York: Macmillan, 1985: 1490–1503.
96. Duckworth W. Insulin degradation: mechanisms, products, and significance. Endocr Rev 1988; 9: 319–345.
97. Duckworth W, Saudek C, Henry R. Why intraperitoneal delivery of insulin with implantable pumps in NIDDM? Diabetes 1992; 41: 657–661.
98. Shapiro D, Blumenkrantz M, Levin S, Coburn J. Absorption and action of insulin added to peritoneal dialysate in dogs. Nephron 1979; 23: 174–180.
99. Scarpioni L, Ballocchi S, Castelli A, Scarpioni R. Insulin therapy in uremic diabetic patients on continuous ambulatory peritoneal dialysis; comparison of intraperitoneal and subcutaneous administration. Perit Dial Int 1994; 14: 127–131.
100. Fuss M, Bergans A, Brauman H. I-125-insulin metabolism in chronic renal failure treated by renal transplantation. Kidney Int 1974; 5: 372–377.
101. Navalesi R, Pilo A, Lenzi S, Donato L. Insulin metabolism in chronic uremia and in the anephric state: effect of the dialytic treatment. J Clin Endocrinol Metab 1975; 40: 70–85.
102. Wideroe T-E, Smeby L, Berg K, Jorstad S, Svart T. Intraperitoneal insulin absorption during intermittent and continuous peritoneal dialysis. Kidney Int 1983; 23: 22–28.
103. Micossi P, Cristallo M, Librenti M. Free-insulin profiles after intraperitoneal, intramuscular, and subcutaneous insulin administration. Diabetes Care 1986; 9: 575–578.
104. Williams G, Pickup J, Clark A, Bowcock S, Cooke E, Keen H. Changes in blood flow close to subcutaneous insulin injection site in stable and brittle diabetics. Diabetes 1983; 32: 466–473.
105. Zingg W, Rappaprot A, Leibel B. Studies on transhepatic absorption. Can J Physiol Pharmacol 1986; 64: 231–234.
106. Selam J-L, Bergman R, Raccah D, Jean-Didier N, Lozano J, Charles M. Determination of portal insulin absorption from peritoneum via novel non-isotopic method. Diabetes 1990; 39: 1361–1365.
107. Tournigand C. Intraperitoneal chemotherapy in ovarian cancer: who and when? Curr Opin Obstet Gynecol 2005; 17: 83–86.
108. Markman M, Reichmann B, Hakes T. Impact on survival of surgically defined favorable responses to salvage intraperitoneal chemotherapy in small-volume residual ovarian cancer. J Clin Oncol 1992; 10: 1479–1484.
109. Sugarbaker P, Graves T, DeBruijn E, et al. Early postoperative intraperitoneal chemotherapy as an adjuvant therapy to surgery for peritoneal carcinomatosis from gastrointestinal cancer: pharmacological studies. Cancer Res 1990; 50: 5790–5794.
110. Kyrgiou M, Salanti G, Pavlidis N, Paraskevaidis E, Ioannidis J. Survival benefits with diverse chemotherapy regimens for ovarian cancer: meta-analysis of multiple treatments. J Natl Cancer Inst 2006; 98: 1655–1663.
111. Farris F, King F, Dedrick R, Litterst CI. Physiological model for the pharmacokinetics of cis-dichlorodiammineplatinum (II) (DDP) in the tumored rat. J Pharmacokinet Biopharm 1985; 13: 13–39.
112. King F, Dedrick R, Farris F. Physiological pharmacokinetic modeling of cis-dichlorodiammineplatinum (II) (DDP) in several species. J Pharmacokinet Biopharm 1986; 14: 131–135.
113. King F, Dedrick R. Physiological pharmacokinetic parameters for cis-dichlorodiammineplatinum (II) (DDP) in the mouse. J Pharmacokinet Biopharm 1992; 20: 95–99.
114. Piccart M, Abrams J, Dodian P, et al. Intraperitoneal chemotherapy with cisplatin and melphalan. J Natl Cancer Inst 1988; 80: 1118–1124.
115. Los G, Mutsaers PHA, van der Vijgh WJF, Baldera GS, de Graag PW, McVie JG. Direct diffusion of cis-diaminedichloroplatinum (II) in intraperitoneal rat tumors after intraperitoneal chemotherapy: a comparison with systemic chemotherapy. Cancer Res 1989; 49: 3380–3384.
116. Dedrick RL, Flessner MF, Collins JM, Schultz JS. Is the peritoneum a membrane? Am Soc Artif Intern Organs J 1982; 5: 1–5.
117. Flessner MF, Fenstermacher JD, Dedrick RL, Blasberg RG. A distributed model of peritoneal-plasma transport: tissue concentration gradients. Am J Physiol 1985; 248: F425–F435.
118. Morrison PF, Dedrick R. Transport of cisplatin in rat brain following microinfusion: an analysis. J Pharm Sci 1986; 75: 120–128.
119. Pretorius R, Petrilli E, Kean C, Ford L, Hoeschele J, Lagasse L. Comparison of the iv and ip routes of cisplatin in dogs. Cancer Treat Rep 1981; 65: 1055–1062.
120. Chabner B. Fluorinated pyrimidines. In: Chabner B, editor. Pharmacologic Principles of Cancer Treatment. Philadelphia: WB Saunders, 1982: 183–212.
121. Collins JM, Dedrick RL, King F, Speyer JL, Myers CE. Nonlinear pharmacokinetic models for 5-fluorouracil in man: intravenous and intraperitoneal routes. Clin Pharmacol Ther 1980; 28: 235–246.
122. Archer S, McCulloch R, Gray B. A comparative study of the pharmacokinetics of continuous portal vein infusion versus intraperitoneal infusion of 5-fluorouracil. Reg Cancer Treat 1989; 2: 105–111.

123. Gianola F, Sugarbaker P, Barofsky I, White D, Myers CE. Toxicity studies of adjuvant intravenous versus intraperitoneal 5-FU in patients with advanced primary colon or rectal cancer. Am J Clin Oncol 1986; 9: 403–410.
124. Penzotti SC, Mattocks AM. Acceleration of peritoneal dialysis by surface active agents. J Pharm Sci 1968; 57: 1192–1195.
125. vanRuth S, Mathot R, Sparidans R, Beijnen J, Verwaal V, Zoetmulder F. Population pharmacokinetics and pharmacodynamics of mitomycin during intraoperative hyperthermic intraperitoneal chemotherapy. Clin Pharmacokinet 2004; 43: 131–143.
126. Witkamp A, deBree E, VanGoethem R, Zoetmulder F. Rationale and techniques of intra-operative hyperthermic intraperitoneal chemotherapy. Cancer Treat Rev 2001; 27: 365–374.
127. Collins JM, Dedrick RL, Flessner MF, Guarino AM. Concentration-dependent disappearance of 5-fluorouracil from peritoneal fluid in the rat: experimental observations and distributed modeling. J Pharm Sci 1982; 71: 735.
128. Flessner MF, Dedrick RL, Schultz JS. A distributed model of peritoneal-plasma transport: theoretical considerations. Am J Physiol 1984; 246: R597–R607.
129. Flessner M.F., Lofthouse J, Zakaria ER. In vivo diffusion of immunoglobulin G in muscle: effects of binding, solute exclusion, and lymphatic removal. Am J Physiol 1997; 273: H2783–H2793.
130. Flessner M.F. Transport of protein in the abdominal wall during intraperitoneal therapy I. Theoretical approach. Am J Physiol Gastrointest Liver Physiol 2001; 281: G424–G437.
131. Baron MA. Structure of the intestinal peritoneum in man. Am J Anat 1941; 69: 439–497.
132. Flessner MF. Net ultrafiltration in peritoneal dialysis: role of direct fluid absorption into peritoneal tissue. Blood Purif 1992; 10: 136–147.
133. Rippe B, Stelin G, Ahlmen J. Frontiers in Peritoneal Dialysis. New York: Field, Rich, 1986.
134. Heimburger O, Waniewski J, Werynski A, Park MS, Lindholm B. Lymphatic absorption in CAPD patients with loss of ultrafiltration capacity. In: Heimburger O, editor. PhD Thesis. Stockholm: Konogl Carolinska Medico Chirurgiska Institute, 1994: 1–21.
135. Daugirdas JT, Ing TS, Gandhi VC, Hano JE, Chen WT, Yuan L. Kinetics of peritoneal fluid absorption in patients with chronic renal failure. J Lab Clin Med 1980; 85: 351–361.
136. Flessner MF. Peritoneal transport physiology: insights from basic research. J Am Soc Nephrol 1991; 2: 122–135.
137. Granger DN, Parker RE, Quillen EW, Brace RA, Taylor AE. Lymphology. Stuttgart, FRG: Thieme, 1979.
138. Courtice FC, Steinbeck AW. Absorption of protein from the peritoneal cavity. J Physiol 1951; 114: 336–355.
139. Flessner M.F., Henegar J, Bigler S, Genous L. Is the peritoneum a significant transport barrier in peritoneal dialysis? Perit Dial Int 2003; 23: 542–549.
140. Vazquez VdL, Stuart OA, Mohamed F, Sugarbaker P. Extent of parietal peritonectomy does not change intraperitoneal chemotherapy pharmacokinetics. Cancer Chemother Rep 2003; 52: 108–112.
141. Hekking LHP, Harvey VS, Havenith CEG, van den Born J, Beelen RHJ, Jackman RW et al. Mesothelial cell transplantation in models of acute inflammation and chronic peritoneal dialysis. Perit Dial Int 2003; 23: 323–330.
142. Margetts PJ, Kolb M, Galt T, Hoff CM, Shockley TR, Gauldie J. Gene transfer of transforming growth factor-Beta1 to the rat peritoneum: effects on membrane function. J Am Soc Nephrol 2001; 12: 2029–2039.
143. Margetts PJ, Gyorffy S, Kolb M, Yu L, Hoff CM, Holmes CJ et al. Antiangiogenic and antifibrotic gene therapy in a chronic infusion model of peritoneal dialysis in rats. J Am Soc Nephrol 2002; 13: 721–728.
144. Jackman RW, Hoff CM, Shockley TR, Nagy JA. Adenovirus-mediated transfer of rat catalase cDNA into rat primary mesothelial cells confers increased resistance to oxidant-induced injury in vitro. J Am Soc Nephrol 1999; 10: 446A–447A.
145. Hoff CM, Piscopo D, Inman K, Shockley TR. Adenovirus-mediated gene transfer to the peritoneal cavity. Perit Dial Int 2000; 20: 128–136.
146. Alvarez RD, Curiel D. A phase I study of recombinant adenovirus vector-mediated intraperitoneal delivery of herpes simplex virus thymidine kinase (HSV-TK) gene and intravenous ganciclovir for previously treated ovarian and extraovarian cancer patients. Hum Gene Ther 1997; 8: 597–613.
147. Mujoo K, Maneval D, Anderson S, Gutterman J. Adenoviral-mediated p53 tumor suppressor gene therapy of human ovarian carcinoma. Oncogene 1996; 12: 1617–1623.
148. Tong X-W, Block A, Chen S-H, Contact C, Agoulnik I, Blankenburg K et al. In vivo gene therapy of ovarian cancer by adenovirus-mediated thymidine kinase gene transduction and ganciclovir administration. Gynecol Oncol 1996; 61: 175–179.
149. deForni M, Boneu A, Otal P, Martel P, Shubinski R, Bugat R et al. Anatomic changes in the abdominal cavity during intraperitoneal chemotherapy: prospective study using scintigraphic peritoneography. Bull Cancer 1993; 80: 345–350.
150. Reed RK, Rubin K, Wiig H, Rodt SA. Blockade of β_1-integrins in skin causes edema through lowering of interstitial fluid pressure. Circ Res 1992; 71: 978–983.
151. Rubin K, Sundberq C, Ahlen K, Reed RK. Integrins: transmembrane links between the extracellular matrix and the cell interior. In: Reed RK, Mattale NG, Bert JL, Winlove CP, Laine GA, editors. Interstitium, Connective Tissue, and Lymphatics. London: Portland Press Ltd, 1995: 29–40.
152. Rubin K, Gullberg D, Tomasini-Johansson B, Reed RK, Ryden C, Borg TK. Molecular recognition of the extracellular matrix by cell surface receptors. In: Comper WD, editor. Extracellular Matrix. Amsterdam: Harwood Academic Publishers, 1996: 262–309.
153. Laurent TC. Structure of the extracellular matrix and the biology of hyaluronan. In: Reed RK, McHale NG, Bert JL, Winlove CP, Laine GA, editors. Interstitium, Connective Tissue, and Lymphatics. London: Portland Press, 1995: 1–12.
154. Fraser JRE, Laurent TC. Hyaluronan. In: Comper WD, editor. Extracellular Matrix. Amsterdam: Harwood Academic Publishers, 1996: 141–199.
155. Wiig H, DeCarlo M, Sibley L, Renkin EM. Interstitial exclusion of albumin in rat tissues measured by a continuous infusion method. Am J Physiol 1992; 263: H1222–H1233.
156. Wiig H, Kaysen GA, Al-Bander HA, DeCarlo M, Sibley L, Renkin EM. Interstitial exclusion of IgG in rat tissues estimated by continuous infusion. Am J Physiol 1994; 266: H212–H219.
157. Zakaria ER, Lofthouse J, Flessner MF. In vivo effects of hydrostatic pressure on interstitium of abdominal wall muscle. Am J Physiol 1999; 276: H517–H529.

158. Zakaria ER, Lofthouse J, Flessner MF. Effect of intraperitoneal pressures on tissue water of the abdominal muscle. Am J Physiol Renal Physiol 2000; 278: F875–F885.
159. Zakaria ER, Lofthouse J, Flessner MF. In vivo hydraulic conductivity of muscle: effects of hydrostatic pressure. Am J Physiol 1997; 273: H2774–H2782.
160. Twardowski ZJ, Prowant BF, Nolph KD. High volume, low frequency continuous ambulatory peritoneal dialysis. Kidney Int 1983; 23: 64–70.
161. Gotloib L, Mines M, Garmizo L, Varka I. Hemodynamic effects of increasing intra-abdominal pressure in peritoneal dialysis. Perit Dial Bull 1981; 1: 41–43.
162. Flessner MF. Osmotic barrier of the parietal peritoneum. Am J Physiol 1994; 267: F861–F870.
163. Flessner MF, Choi J, Credit K, Deverkadra R, Henderson K. Resistance of tumor interstitial pressure to the penetration of intraperitoneally delivered antibodies into metastatic ovarian tumors. Clin Cancer Res 2005; 11: 3117–3125.
164. Flessner MF, Dedrick RL, Reynolds JC. Bidirectional peritoneal transport of immunoglobulin in rats: tissue concentration profiles. Am J Physiol 1992; 263: F15–F23.
165. Flessner MF. Changes in the peritoneal interstitium and their effect on peritoneal transport. Perit Dial Int 1999; 19 Suppl 2: S77–S82.
166. Flessner MF. The transport barrier in intraperitoneal therapy. Am J Physiol 2005; 288: F433–F442.
167. Wiig H, Reed RK, Aukland K. Micropuncture measurement of interstitial fluid pressure in rat subcutis and skeletal muscle: comparison to the wick-in-needle technique. Microvasc Res 1981; 21: 308–319.
168. Wiig H, Reed RK. Interstitial compliance and transcapillary Starling pressures in cat skin and skeletal muscle. Am J Physiol 1985; 248: H666–H673.
169. Flessner MF, Choi J, He Z, Credit K. Physiological characterization of human ovarian cancer cells in a rat model of intraperitoneal antineoplastic therapy. J Appl Physiol 2004; 97: 1518–1526.
170. Boucher Y, Baxter LT, Jain RK. Interstitial pressure gradients in tissue-isolated and subcutaneous tumors: implications for therapy. Cancer Res 1990; 50: 4478–4484.
171. Boucher Y, Kirkwood JM, Opacic D, Desantis M, Jain RK. Interstitial hypertension in superficial metastatic melanomas in humans. Cancer Res 1991; 51: 6691–6694.
172. Roh HD, Boucher Y, Kalnicki S, Buchsbaum R, Bloomer WD, Jain RK. Interstitial hypertension in carcinoma of uterine cervix in patients: possible correlation with tumor oxygenation and radiation exposure. Cancer Res 1991; 51: 6695–6698.
173. Gullino PM, Grantham FH, Smith SH. The interstitial water space of tumors. Cancer Res 1965; 25: 727–731.
174. Boucher Y, Jain R.K. Microvascular pressure is the principal driving force for interstitial hypertension in solid tumors: implications for vascular collapse. Cancer Res 1992; 52: 5110–5114.
175. Jain RK. Transport of molecules in the tumor interstitium: a review. Cancer Res 1987; 47: 3039–3051.
176. Netti PA, Berk DA, Swartz MA, Grodzinsky AJ, Jain RK. Role of extracellular matrix assembly in interstitial transport in solid tumors. Cancer Res 2000; 60: 2497–2503.
177. Choi J, Credit K, Henderson K, Deverkadra R, He Z, Wiig H et al. Intraperitoneal immunotherapy for metastatic ovarian carcinoma: resistance of intratumoral collagen to antibody penetration. Clin Cancer Res 2006; 12: 1906–1912.
178. Vink H, Duling BR. Identification of distinct luminal domains for macromolecules, erythrocytes, and leucocytes within mammalian capillaries. Circ Res 1996; 79: 581–589.
179. Vink H, Duling BR. Capillary endothelial surface layer selectively reduces plasma solute distribution volume. Am J Physiol 2000; 278: H285–H289.
180. Fu B, Curry FE, Adamson RH, Weinbaum S. A model for interpreting the tracer labeling of interendothelial clefts. Ann Biomed Eng 1997; 25: 375–397.
181. Fu BM, Curry FE, Weinbaum S. A diffusion wake model for tracer ultrastructure-permeability studies in microvessels. Am J Physiol 1995; 269: H2124–H2140.
182. Platts SH, Duling BR. Adenosine A3 receptor activation modulates the capillary endothelial glycocalyx. Circ Res 2004; 94: 77–82.
183. Matsuki T, Duling B. TNF-alpha increases entry of macromolecules into luminal endothelial cell glycocalyx. Microcirculation 2000; 7: 411–418.
184. Leunig M, Yuan F, Menger MD, Boucher Y, Goetz AE, Messmer K et al. Angiogenesis, microvascular architecture, microhemodynamics, and interstitial fluid pressure during early growth of human adenocarcinoma LS174T in SCID mice. Cancer Res 1992; 52: 6553–6560.
185. Nugent LJ, Jain RK. Plasma pharmacokinetics and interstitial diffusion of macromolecules in a capillary bed. Am J Physiol 1984; 246: H129–H137.
186. Yuan F, Leunig M, Berk DA, Jain RK. Microvascular permeability of albumin, vascular surface area, and vascular volume measured in human adenocarcinoma LS174T using dorsal chamber in SCID mice. Microvasc Res 1993; 45: 269–289.
187. Gerlowski LE, Jain RK. Microvascular permeability of normal and neoplastic tissues. Microvasc Res 1986; 31: 288–305.
188. Henry CBS, Duling BR. TNF-alpha increases entry of macromolecules into luminal endothelial cell glycocalyx. Am J Physiol 2000; 279: H2815–H2823.
189. Bettendorf U. Electronmicroscopic studies on the peritoneal resorption of intraperitoneally injected latex particles via the diaphragmatic lymphatics. Lymphology 1979; 12: 66–70.
190. Courtice FC, Steinbeck AW. The effects of lymphatic obstruction and of posture on absorption of protein from the peritoneal cavity. Aust J Exp Biol Med Sci 1951; 29: 451–458.
191. Dykes PW, Jones JH. Albumin exchange between plasma and ascites fluid. Clin Sci 1964; 34: 185–197.
192. Rusznysk I, et al. Lymphatics and Lymph Circulation. London: Pergamon Press, 1967.
193. Baxter LT, Jain RK. Transport of fluid and macromolecules in tumor. I. Role of interstitial pressure and convection. Microvasc Res 1989; 37: 77–104.
194. Flessner MF, Deverkadra R, Smitherman J, Li X, Credit K. In vivo determination of diffusive transport parameters in a superfused tissue. Am J Physiol Renal Physiol 2006; 291: F1096–F1103.

195. Ward BG, Mather SJ, Hawkins LR, Crowther ME, Shepherd JH, Granowska M et al. Localization of radioiodine conjugated to the monoclonal antibody HMFG2 in human ovarian carcinoma: assessment of intravenous and intraperitoneal routes of administration. Cancer Res 1987; 47: 4719–4723.
196. Dedrick RL, Flessner MF. Pharmacokinetic considerations on monoclonal antibodies. In: M. Mitchell (ed.). Immunity to Cancer II. Proc. of 2nd conference on Immunity to Cancer. Williamsburg, VA,1989; II: 429–438.
197. Krediet RT, Struijk DG, Koomen GCM. Peritoneal transport of macromolecules in patients on CAPD. Contrib Nephrol 1991; 89: 161–174.
198. Griffin T, Collins JA, Bokhari F. Intraperitoneal immunoconjugates. Cancer Res 1990; 50: 1031–1038.
199. Clauss MA, Jain RK. Interstitial transport of rabbit and sheep antibodies in normal and neoplastic tissues. Cancer Res 1990; 30: 3487–3492.
200. Berk DA, Yuan F, Leunig M, Jain RK. Direct in vivo measurement of targeted binding in a human tumor xenograft. Proc Natl Acad Sci U S A 1997; 94 (5): 1785–1790.
201. Fujimori K, Covell DG, Fletcher JE, Weinstein JN. Modeling analysis of the global and microscopic distribution of immunoglobulin G, F(ab')$_2$ and Fab in tumors. Cancer Res 1989; 49: 5656–5663.
202. Fujimori K, Covell DG, Fletcher J, Weinstein J. A modeling analysis of monoclonal antibody percolation through tumors: a binding-site barrier. J Nucl Med 1990; 31: 1191–1198.
203. van Osdol W, Fujimori K, Weinstein JN. An analysis of monoclonal antibody distribution in microscopic tumor nodules: consequences of a 'binding site barrier'. Cancer Res 1991; 51: 4776–4784.
204. Flessner MF, Dedrick RL. Tissue-level transport mechanisms of intraperitoneally-administered monoclonal antibodies. J Control Release 1998; 53: 69–75.
205. Rippe B, Haraldsson B. Fluid and protein fluxes across small and large pores in the microvasculature. Application of two-pore equations. Acta Physiol Scand 1987; 131: 411–428.
206. Flessner MF, Dedrick RL. Monoclonal antibody delivery to intraperitoneal tumors in rats: effects of route of administration and intraperitoneal solution osmolality. Cancer Res 1994; 54: 4376–4384.